Full title: Guanidine hydrochloride reactivates an ancient septin hetero-oligomer assembly pathway in budding yeast

Short title: Septin protein complex assembly and evolution

Courtney R. Johnson[1], Marc G. Steingesser[1], Andrew D. Weems[1], Anum Khan[2], Amy Gladfelter[2], Aurélie Bertin[3,4] and Michael A. McMurray[1,*]

[1]Department of Cell and Developmental Biology, University of Colorado Anschutz Medical Campus, Aurora, CO 80045 USA

[2]Department of Biology, University of North Carolina at Chapel Hill, Chapel Hill, NC 27599 USA

[3]Laboratoire Physico Chimie Curie, Institut Curie, PSL Research University, CNRS UMR 168, 75005, Paris, France.

[4]Sorbonne Université UPMC Univ Paris 06, 75005, Paris, France

*Corresponding author

E-mail: michael.mcmurray@cuanschutz.edu

ABSTRACT

Septin proteins co-assemble into hetero-oligomers that polymerize into cytoskeletal filaments with a variety of cellular functions. In *Saccharomyces cerevisiae*, where septins were first discovered, five subunits comprise two species of septin hetero-octamers, Cdc11/Shs1–Cdc12–Cdc3–Cdc10–Cdc10–Cdc3–Cdc12–Cdc11/Shs1. Septins evolved from ancestral GTPases. We previously found evidence that slow GTPase activity by Cdc12 directs the choice of incorporation of Cdc11 vs Shs1 into septin complexes. It was unclear why many septins, including Cdc3, lack GTPase activity. We serendipitously discovered that the small molecule guanidine hydrochloride (GdnHCl) rescues septin function in *cdc10* mutants by promoting assembly of non-native Cdc11/Shs1–Cdc12–Cdc3–Cdc3–Cdc12–Cdc11/Shs1 hexamers. We provide evidence that in *S. cerevisiae* Cdc3 guanidinium ion (Gdm) occupies the site of a “missing” Arg sidechain that is present in other fungal species in which (i) the Cdc3 subunit is an active GTPase and (ii) Cdc10-less hexamers co-exist with octamers in wild-type cells. These findings support a model in which Gdm reactivates a latent septin assembly pathway that was suppressed during fungal evolution in order to restrict assembly to hetero-octamers. Given that septin hexamers made natively in human cells also exclude Cdc10-like central subunits via homodimerization of an active GTPase, our results provide new mechanistic details that likely apply to septin assembly throughout phylogeny.

INTRODUCTION

Septin proteins are found in nearly every eukaryotic lineage, with the exception of land plants (Auxier, Dee, Berbee, & Momany, 2019; Nishihama, Onishi, & Pringle, 2011; Onishi & Pringle, 2016; Pan, Malmberg, & Momany, 2007). In most extant organisms studied to date, multiple septin proteins co-assemble into linear, rod-shaped hetero-oligomers with at least some potential to polymerize into filaments (Fung, Dai, & Trimble, 2014; Mostowy & Cossart, 2012; Y. Oh & Bi, 2011). Septin hetero-oligomers are now known to contribute functionally to a wide variety of cellular processes (Dolat, Hu, & Spiliotis, 2014; Saarikangas & Barral, 2011). A number of human diseases and disorders, ranging from cancer to male infertility, have been linked to septin dysregulation or mutation (Dolat et al., 2014; Saarikangas & Barral, 2011), but within our understanding of septin roles in cellular function one common theme emerges: the ability to assemble into quaternary complexes is key.

All distinct septins share clear homology, but phylogenetic analysis reveals septin groups and subgroups (Pan et al., 2007) that can accurately predict which septin occupies which subunit position within hetero-oligomers (Nakahira et al., 2010). However, the subtleties of the distinctions between septins that drive assembly of hetero-oligomers with precise subunit organization remain incompletely understood. Moreover, the oligomerization interfaces have not diverged drastically from the ancestral form, as nearly all septins retain the ability to homo-oligomerize *in vitro* (Farkasovsky, Herter, Voss, & Wittinghofer, 2005; Versele et al., 2004) whether or not they do so *in vivo*. How cells assemble specific septin hetero-oligomers to meet functional demands represents a major focus of septin research. More generally, septins provide a powerful model to study the mechanisms by which multisubunit complexes are assembled with high efficiency and fidelity in living cells.

Septins clearly evolved from an ancestral GTPase (Leipe, Wolf, Koonin, & Aravind, 2002) but multiple septins subsequently lost the ability to hydrolyze GTP. Unlike the building blocks of polymers of the other cytoskeletal NTPases actin and tubulin (and their prokaryotic counterparts), in native septin hetero-oligomers most, if not all, of the septin nucleotide-binding pockets are buried within an oligomerization interface, called the G interface (Sirajuddin et al., 2007). Particularly for septin complexes in budding yeast, where hetero-octamers polymerize into filaments via the other, so-called "NC" septin-septin interface (Bertin et al., 2008; Sirajuddin et al., 2007), burial of GTP in G interfaces within highly stable complexes severely limits the potential for cycles of GTP binding, hydrolysis, and exchange to modulate the assembly and disassembly of septin filaments. Nonetheless, most septins retain sequences clearly corresponding to regions/motifs in other small GTPases that contact bound nucleotide and/or change conformation upon GTP hydrolysis. These include the G1/Walker/P-loop, residues of which contact each of the three phosphates; the G2/Switch I and G3/Switch II loops, which are in proximity to the γ phosphate when it is present but are in distinct locations when it is absent; and the G4 motif, which contacts the base and dictates specificity for guanosine nucleotides. The question of what roles GTP binding and hydrolysis play in septin biogenesis and function has been a major focus in septin research for over two decades (Mitchison & Field, 2002).

The baker's yeast, *Saccharomyces cerevisiae*, has been at the forefront of septin research, for a number of reasons. The repertoire of septin proteins expressed in yeast (seven) is much simpler than that of humans (13). Two yeast septins are expressed and function specifically during the process of sporulation (De Virgilio, DeMarini, & Pringle, 1996; Fares, Goetsch, & Pringle, 1996; Garcia et al., 2016; Heasley & McMurray, 2016; Pablo-Hernando et al., 2008), a version of gametogenesis, leaving five septins expressed in nearly stoichiometric amounts (Kulak, Pichler, Paron, Nagaraj, & Mann, 2014) in mitotically dividing cells: Cdc3, Cdc10, Cdc11, Cdc12, and Shs1. Yeast septin localization during the mitotic cell division cycle is primarily restricted to the cortex,

where the septins take the form of filamentous rings at the mother-bud neck that undergo a series of discrete structural transitions as the bud emerges and grows and cytokinesis and cell separation take place (Y. Oh & Bi, 2011). Septin filament assembly is essential for proliferation (McMurray et al., 2011), and septin ring assembly, bud morphogenesis and cytokinesis are grossly perturbed in viable septin mutants (Hartwell, 1971), providing clear readouts for defects in septin biogenesis (McMurray, 2016). A combination of molecular genetic (Garcia et al., 2011; Iwase, Luo, Bi, & Toh-e, 2007; McMurray et al., 2011; Nagaraj, Rajendran, Jackson, & Longtine, 2008; Versele et al., 2004), biochemical (Bertin et al., 2008; Farkasovsky et al., 2005; Garcia et al., 2011; Versele et al., 2004), and structural (Bertin et al., 2008; Farkasovsky et al., 2005; Garcia et al., 2011; Sirajuddin et al., 2007) approaches have demonstrated that two kinds of hetero-octamers co-exist, with a linear hexameric core of the order Cdc12–Cdc3–Cdc10–Cdc10–Cdc3–Cdc12 “capped” at each end with either Cdc11 or Shs1. While the functional basis for yeast octamer diversity remains largely unknown, at the level of quaternary structure septins are best understood in *S. cerevisiae*.

We are most interested in the mechanisms of assembly of septin hetero-oligomers, and previously used mutants isolated in unbiased genetic screens to elucidate roles in this process for nucleotide binding (A. D. Weems, Johnson, Argueso, & McMurray, 2014) and interactions with cytosolic chaperones (Johnson, Weems, Brewer, Thorner, & McMurray, 2015), including the fungal disaggregase Hsp104, a hexameric AAA+ ATPase (Sweeny & Shorter, 2016). Here we report that the function of specific septin mutants is affected in unexpected ways by guanidine hydrochloride (GdnHCl), a small molecule used for decades to inhibit Hsp104 ATPase activity *in vivo* (Derkatch, Bradley, Zhou, Chernoff, & Liebman, 1997; Jung & Masison, 2001). Our findings reveal important roles for specific residues and structural motifs in septin hetero-oligomer assembly, suggest a series of key events during fungal septin evolution that enforced incorporation of Cdc10 subunits in hetero-oligomers, and provide what is, to our knowledge, the first evidence that guanidinium (Gdm) has the potential to functionally replace Arg residues *in vivo*.

113

114 RESULTS

115 **GdnHCl restores high-temperature septin function to *cdc10* mutants in an Hsp104-**
116 **independent manner**

117 We previously reported interactions between an ATPase-dead mutant of Hsp104 and a
118 temperature-sensitive (TS) mutant of Cdc10, in which overexpression of the mutant Hsp104
119 inhibited the proliferation of *cdc10(D182N)* cells at an otherwise permissive low temperature (27ºC)
120 (Johnson et al., 2015). We expected that the addition of 3 mM GdnHCl to the culture medium would
121 mimic these inhibitory effects in cells with wild-type (WT) Hsp104. Instead, we found complete
122 rescue by GdnHCl of the *cdc10(D182N)* TS proliferation defect at all temperatures tested (up to
123 37ºC) (Figure 1A). GdnHCl did not have the same effect on cells carrying TS alleles of other septins,
124 although in its presence a *cdc3(G365R)* strain grew noticeably worse at 27 ºC, 30 ºC and 34 ºC,
125 and a *cdc12(G247E)* strain grew slightly worse at 30ºC and slightly better at 37ºC (Figure 1A). To
126 our surprise, GdnHCl rescue of *cdc10(D182N)* did not require Hsp104 (Figure 1B). Others have
127 suggested that a mitochondrial Hsp104 homolog, Hsp78, might share functions with Hsp104 (Erives
128 & Fassler, 2015), and Hsp78 and Hsp104 share the same residues within the ATP binding pocket
129 that contact Gdm in the bacterial Hsp104 homolog ClpB (Figure 1C), but Hsp78 was also
130 dispensable for GdnHCl rescue of *cdc10(D182N)* high-temperature growth (Figure 1B). Inhibition of
131 Hsp104 (i.e., curing of prions) or Hsp78 (i.e., induction of cytoplasmic petites) by GdnHCl *in vivo*
132 requires concentrations in the medium of ≥1 mM (Tuite, Mundy, & Cox, 1981), but GdnHCl was
133 sufficient to provide partial rescue of 37ºC growth by *cdc10(D182N)* cells at concentrations <0.1
134 mM (Figure 1D,E). We conclude that GdnHCl suppresses septin defects in *cdc10(D182N)* mutants
135 via a mechanism that does not involve Hsp104 or its homolog Hsp78.

136

137 **GdnHCl drives exclusion of mutant Cdc10 molecules from higher-order septin structures**

138 We previously noted that the *cdc12(G247E)* mutation appears to decrease the levels of WT Cdc10
139 (Johnson et al., 2015). Cells tolerate loss of Cdc10 by assembling filaments via hexameric building
140 blocks in which Cdc3 forms a non-native G homodimer, but *cdc10Δ* cells are TS, presumably
141 because at high temperature Cdc3 fails to adopt the homodimerization-competent conformation
142 and/or the non-native Cdc3 homodimer is unstable (McMurray et al., 2011). Rescue of the TS
143 defects at 37ºC of the *cdc10(D182N)* and *cdc12(G247E)* mutants by GdnHCl could reflect improved
144 assembly of Cdc10-less hexamers, rather than any specific effect on the *cdc10(D182N)* allele.
145 Consistent with this idea, GdnHCl also fully suppressed the TS phenotype resulting from a G100E
146 substitution in Cdc10 (Figure 1–figure supplement 1A), as well as that of *cdc10Δ* (Figure 2A). Clear
147 but partial GdnHCl rescue was also observed for *cdc10(G44D)* cells (Figure 1–figure supplement
148 1A). We confirmed via immunofluorescence with anti-Cdc11 antibodies (Figure 1–figure supplement
149 1B) and electron microscopy (Figure 1–figure supplement 1C) that at 37ºC GdnHCl-treated *cdc10*
150 cells assembled filamentous rings composed of other septins. Thus GdnHCl does not simply bypass
151 the need for septin filaments.
152
153 Given these results, we wondered if in cells carrying point-mutant *cdc10* alleles GdnHCl bypasses
154 altogether the incorporation of the mutant Cdc10 subunits during septin hetero-oligomer assembly.
155 Indeed, even at temperatures permissive in the absence of GdnHCl for septin ring incorporation of
156 Cdc10(D182N)-GFP, in the presence of 3 mM GdnHCl the fluorescence of Cdc10(D182N)-GFP
157 was restricted to the cytoplasm (Figure 2B). WT Cdc10-GFP continued to localize to the bud neck
158 despite the presence of GdnHCl (Figure 2B). Similarly, in diploid cells co-expressing Cdc10-
159 mCherry and Cdc10(D182N)-GFP, the addition of GdnHCl specifically eliminated Cdc10(D182N)
160 incorporation in septin rings, with no obvious effect on WT Cdc10 (Figure 2C). Our results suggest
161 that when mutations within the Cdc10 G interface perturb the ability of Cdc10 to acquire a

162 conformation that binds tightly to Cdc3, GdnHCl allows other Cdc3 molecules to outcompete the
163 mutant Cdc10 proteins for occupancy of the Cdc3 G interface, ultimately co-assembling with Cdc11,
164 Cdc12, and Shs1 into Cdc10-less hexamers capable of robust septin functions. As predicted from
165 this model, GdnHCl was unable to rescue *cdc10Δ* growth when Cdc3 carried a mutation (W364A)
166 previously shown (McMurray et al., 2011) to block Cdc3 homodimerization (Figure 2D).
167
168 **GdnHCl promotes Cdc10-less filament assembly *in vitro* by purified, recombinant complexes**
169 Yeast septin function is regulated (in poorly defined ways) by a large number of pathways (Longtine
170 & Bi, 2003), which might be altered by GdnHCl to indirectly promote Cdc3 homodimerization.
171 GdnHCl might also alter other properties of Cdc10-less yeast cells to promote septin function
172 despite inefficient Cdc3 homodimerization. For example, deletion of *DPL1*, which encodes a
173 dihydrosphingosine phosphate lyase, improves the proliferation of *cdc10*Δ cells at the moderate
174 temperature of 30ºC (Michel et al., 2017). The authors of that study speculated that the absence of
175 Dpl1 alters the properties of the plasma membrane in ways that mimic the effects of low temperature
176 and allow Cdc10-less septin complexes to better function in cytokinesis (Michel et al., 2017).
177 Accordingly, Cdc10-less septin function at high-temperature in the presence of GdnHCl might reflect
178 GdnHCl inhibition of Dpl1. However, *cdc10*Δ *dpl1*Δ cells were only able to proliferate at 37ºC when
179 GdnHCl was present in the growth medium (Figure 1–figure supplement 1D). While these data do
180 not exclude the possibility that GdnHCl alters membrane properties in ways independent of Dpl1,
181 they demonstrate that the GdnHCl effect on septin function in *cdc10*Δ cells is Dpl1-independent.
182
183 To ask if GdnHCl is able to promote Cdc10-less septin filament assembly outside of yeast cells and
184 away from membranes, we co-expressed Cdc3, Cdc11, and hexahistidine-tagged Cdc12 (6xHis-
185 Cdc12) in *E. coli*, which lacks native septins, and purified septin complexes as described previously
186 (McMurray et al., 2011). We then used negative staining and electron microscopy (EM) to ask if

187 these purified complexes appeared as hexamers in high-salt solution and polymerized into filaments
188 upon salt dilution. We previously used the same approach to demonstrate that a mutation in the
189 Cdc3 G interface, G261V, promotes septin hexamer and filament assembly in the absence of Cdc10
190 (McMurray et al., 2011). To test effects of GdnHCl, we either grew the bacteria in the presence of
191 50 mM GdnHCl and kept GdnHCl in all buffers thereafter, or we only introduced the GdnHCl during
192 purification. In the absence of GdnHCl, Cdc10-less complexes were detected in high salt as particles
193 of two or three septins (Figure 3A), and were unable to polymerize into filaments in low salt (Figure
194 3B), consistent with our earlier work (McMurray et al., 2011). Two-septin particles likely represent
195 Cdc3–Cdc12 hetero-dimers, since in these conditions Cdc11 occasionally dissociates from the ends
196 of hetero-octamers containing Cdc10 (Bertin et al., 2008). Complexes synthesized in the presence
197 of GdnHCl, on the other hand, were found in high salt as trimers, tetramers, pentamers and
198 hexamers (Figure 3A). The larger complexes were frequently "kinked" at a location three subunits
199 from one end (Figure 3A), consistent with weak septin-septin contacts at this point, which we also
200 previously observed with the Cdc3(G261V) mutation (McMurray et al., 2011). Upon salt dilution,
201 these complexes robustly polymerized into bundles of laterally-associated filaments (Figure 3B),
202 very similar to the behavior of WT hetero-octamers that contain Cdc10 (Bertin et al., 2008). Fourier
203 transform analysis of the striations in these filament bundles revealed a repeating unit of ~27 nm,
204 the length of a septin hexamer (Figure 3B). Adding GdnHCl to complexes synthesized in its absence
205 did not allow filament formation (Figure 3C). We conclude from these data that GdnHCl is able to
206 promote septin filament assembly by recombinant Cdc10-less septin complexes produced in a
207 heterologous system that lacks septin-regulatory pathways. Thus GdnHCl likely acts directly on
208 septin proteins, and only when it is present during septin folding/assembly.
209

210 **Unbiased *in silico* modeling and phylogenetic analysis point to Thr302 as the site of Gdm**
211 **binding in Cdc3**

212 We identified the G261V mutation in Cdc3 using an unbiased genetic selection for suppressors of
213 the TS phenotype of *cdc10*Δ cells, and concluded that the introduction of Val in this position
214 stabilizes a conformation of the G interface that self-associates better than the major conformation
215 populated by WT Cdc3 at high temperatures (McMurray et al., 2011). We reasoned that Gdm might
216 bind in the Cdc3 G interface and similarly promote the homodimerization-competent conformation.
217 For clues as to where Gdm might bind, we first used the structure of human SEPT2 bound to the
218 non-hydrolyzable nucleotide analog 5'-guanylyl imidodiphosphate (GppNHp) (Sirajuddin,
219 Farkasovsky, Zent, & Wittinghofer, 2009) to generate a homology model of the globular domain of
220 monomeric Cdc3, and then performed unbiased *in silico* docking simulations to ask for the lowest-
221 energy predicted sites of Gdm binding. Four sites had binding free energies of ≤-3 kcal/mol. One
222 site, between the sidechains of Thr302 and His262, lies in the G interface, and had the second-
223 lowest predicted free energy of binding (Figure 4A).
224
225 As a parallel approach, we considered that (i) Gdm mimics the distal end of an Arg sidechain, and
226 (ii) a number of previous *in vitro* studies of diverse non-septin proteins – including T4 lysozyme
227 (Baldwin, Baase, Zhang, Feher, & Matthews, 1998), β-galactosidase (Dugdale et al., 2010), and
228 carboxypeptidase A (Phillips, Hedstrom, & Rutter, 1992) – demonstrated that Gdm is able to
229 functionally occupy molecular vacancies that are created by the replacement of an Arg residue with
230 residues having smaller sidechains (e.g. Ala). We thus hypothesized that one or more Arg residues
231 might contribute to G interface contacts for other septins that are, unlike *S. cerevisiae* Cdc3, capable
232 of robust G homodimerization.
233
234 To identify candidate Arg residues, we performed a phylogenetic analysis of Cdc3 homologs from
235 different species, which we separated into two categories based on the severity of phenotypes
236 accompanying deletion of the *CDC10* homolog. If non-*Saccharomyces* species possess an Arg that
237 favors G homodimerization by Cdc3, then we predicted this group of species should easily form

238 Cdc10-less septin hexamers and be better able to tolerate deletion of the Cdc10 homolog. Such
239 functional information was available for non-*Saccharomyces* species from eleven distinct fungal
240 genera. In *Aspergillus* (*fumigatis* (Vargas-Muñiz et al., 2015) or *nidulans* (Hernández-Rodríguez,
241 Hastings, & Momany, 2012)), *Candida albicans* (Warenda & Konopka, 2002), *Cryptococcus*
242 *neoformans* (Kozubowski & Heitman, 2010), *Fusarium graminearum* (Chen et al., 2016),
243 *Neurospora crassa* (Berepiki & Read, 2013), *Schizosaccharomyces pombe* (An, Morrell, Jennings,
244 Link, & Gould, 2004), and *Ustilago maydis* (Alvarez-Tabarés & Pérez-Martín, 2010), deletion of the
245 Cdc10 homolog has distinctly milder phenotypic consequences compared to deletion of the Cdc3
246 homolog. In *Magnaporthe oryzae*, septin ring assembly is perturbed by deletion of any septin, but
247 higher-order, filamentous structures persist in cells lacking the Cdc10 homolog Sep4, whereas in
248 the other mutants septin localization is almost exclusively diffuse (Dagdas et al., 2012). Finally, in
249 *Coprinopsis cinerea*, a UV-induced mutant defective in fruiting body development was rescued by
250 a gene encoding CcCdc3, but the expression of CcCdc10 remained about 100-fold decreased in
251 the mutant following rescue, suggesting that the mutant was defective in both CcCdc3 and CcCdc10
252 expression, and that rescue of CcCdc3 expression was sufficient to restore function (Shioya et al.,
253 2013). We interpret these results as evidence that in *C. cinerea*, as well, loss of Cdc10 is better
254 tolerated than loss of Cdc3.
255
256 By contrast, only the Shs1 homolog is non-essential for proliferation in *Kluyveromyces lactis*
257 (Rippert & Heinisch, 2016). In *Ashbya gossypii*, deletion of any mitotic septin prevents septin ring
258 assembly; loss of the Cdc10 homolog is as severe as loss of the Cdc3 homolog (Helfer & Gladfelter,
259 2006). According to our hypothesis, if there is a key Arg residue that promotes Cdc3
260 homodimerization, and *S. cerevisiae* lacks it, then *K. lactis* and *A. gossypii* should also lack it.
261
262 Figure 4–figure supplement 1 shows an alignment of protein sequences for Cdc3 homologs from
263 the fungal species listed above. As ScCdc3 is predicted to be unable to hydrolyze GTP (Sirajuddin

264 et al., 2009), we also included for comparison human SEPT2 and SEPT9, because for these septins
265 crystal structures are available of non-native G homodimers in the "GTP state" (bound to the non-
266 hydrolyzable GTP analogs GppNHp or GTPγS, respectively). Only 16 residues were distinctly
267 different between a group including *S. cerevisiae* and the two species that cannot tolerate Cdc10
268 loss, and the group of species that tolerate *CDC10* deletion. For six of these residues, the changes
269 reflect substitutions with strong predicted effects on amino acid properties (polarity, charge, size,
270 etc.). One of these non-conservative variants lies in the C-terminal extension, which is disordered
271 in septin crystal structures. Based on the crystal structures of SEPT2•GppNHp and SEPT9•GTPγS,
272 all of the other five non-conservative variants cluster near the G interface (Figure 4B), and one of
273 these residues – corresponding to Thr302 in ScCdc3 – is an Arg in eight of the nine species that
274 tolerate Cdc10 loss (Figure 4–figure supplement 1). Moreover, in the SEPT2•GppNHp structure the
275 Gdm group of the corresponding Arg in SEPT2 is located in the same place where our *in silico*
276 docking results predicted that Gdm binds to Cdc3, between Thr302 and His262 (Figure 4). Together,
277 these findings strongly support the idea that Gdm promotes Cdc3 homodimerization by occupying
278 the same site in the Cdc3 G interface that in other septins is occupied by the Gdm moiety of an Arg
279 sidechain. This Arg residue was likely substituted to Thr during the evolution of the fungal lineage
280 that includes *S. cerevisiae*, *A. gossypii*, and *K. lactis*, concomitant with loss of Cdc10-less hexamers
281 in these yeasts.
282

283 **GdnHCl promotes higher-order septin assembly in *A. gossypii* cells lacking Cdc10**

284 Our phylogenetic comparisons predicted that Gdm should act similarly on the *A. gossypii* Cdc3
285 homolog to promote AgCdc3 homodimerization in the absence of Cdc10. To test this prediction, we
286 exposed *A. gossypii* cells lacking *CDC10* to GdnHCl and assessed higher-order septin assembly
287 by monitoring the localization of Shs1-GFP expressed in the same cells. As reported previously
288 (Helfer & Gladfelter, 2006), in *cdc10*Δ cells in the absence of GdnHCl Shs1-GFP fluorescence was

289 cytoplasmic and diffuse (Figure 5). Addition of GdnHCl restored the localization of Shs1-GFP to
290 branch points and hyphal tips (Figure 5), the same pattern observed in WT cells (Helfer & Gladfelter,
291 2006). Thus the ability of GdnHCl to promote septin function in the absence of Cdc10, and the loss
292 of Arg at the position corresponding to ScCdc3 Thr302, are both conserved over >100m years of
293 evolution.
294
295 **Chemical rescue of *cdc10* by Gdm derivatives**
296 To better understand the molecular details of Gdm "rescue" of Arg-substituted mutants, earlier *in*
297 *vitro* Gdm studies also tested other small molecules with similar chemical properties, including urea
298 and the GdnHCl derivatives aminoguanidine (Pimagedine, here "aGdnHCl") and N-ethylguanidine
299 ("eGdnHCl") (Rynkiewicz & Seaton, 1996). We undertook an analogous approach to study GdnHCl
300 rescue of the *cdc10* TS phenotype.
301
302 First, we tested urea, which differs from Gdm by only a few atoms (Figure 6A). We grew WT or
303 *cdc10* cells on solid rich medium containing 0.64 M urea, a concentration we found to slow, but not
304 prevent, growth of WT cells, and saw no *cdc10* rescue (Figure 6A-B). To test a range of
305 concentrations, we also placed filter disks soaked with GdnHCl or urea on lawns of WT or *cdc10*
306 cells. We saw a clear zone of rescue around the GdnHCl disk, but not with urea (Figure 6C). We
307 next exposed WT or *cdc10* cells to 0.375 mM GdnHCl, aGdnHCl, eGdnHCl, or combinations of
308 GdnHCl plus eGdnHCl or GdnHCl plus aGdnHCl (0.375 mM each). At 0.375 mM GdnHCl provided
309 only a partial rescue (Figure 6D), allowing us to detect subtle effects of the GdnHCl derivatives when
310 combined with GdnHCl. At 22ºC, 0.375 mM of any single drug had no noticeable effect on growth;
311 slight growth inhibition of both WT and mutant cells was observed when the total concentration of
312 GdnHCl plus derivative was 0.75 mM (Figure 6D). At 37ºC, in addition to the expected partial *cdc10*
313 rescue by GdnHCl, there was a very slight rescue by eGdnHCl, and an even less pronounced
314 rescue by aGdnHCl (Figure 6D). By contrast, mixing GdnHCl with aGdnHCl or eGdnHCl to a total

315 concentration of 0.75 mM resulted in full or nearly full rescue of *cdc10* 37ºC growth, respectively
316 (Figure 6D). We interpret these findings to mean that aGdm and eGdm (the guanidinium ion
317 derivatives) occupy the position between Cdc3 Thr302 and His262 differently than does Gdm. They
318 may not provide the appropriate molecular contacts across the G dimer interface, or they may bind
319 less well, or even too well (if Gdm acts only transiently during Cdc3 folding). Indeed, aGdm and
320 eGdm were predicted by *in silico* modeling to bind in the same location as Gdm but with lower free
321 energies, with the additional moieties projecting in various directions (Figure 6E) in ways that might
322 further alter Cdc3 conformation. It is also possible that yeast cells are less permeable to these
323 GdnHCl derivatives. Urea does not rescue at all, possibly because it cannot form a cation. Finally,
324 as would be expected if only small molecules like Gdm can fit into the pocket provided by Thr302
325 and surrounding residues, 5 mM arginine hydrochloride in the medium provided no *cdc10* rescue
326 (Figure 6F).
327
328 **Mutating Cdc3 Thr302 to Arg prevents *cdc10*Δ rescue by GdnHCl**
329 To test if the absence of Arg at ScCdc3 position 302 is sufficient to explain the inability of *S.*
330 *cerevisiae cdc10*Δ cells to proliferate at 37ºC, we replaced Thr302 with Arg. The double-mutant
331 *cdc10*Δ *cdc3(T302R)* cells were, like *cdc10*Δ *CDC3*$^+$, TS, but unlike *cdc10*Δ *CDC3*$^+$ the addition of
332 GdnHCl failed to restore proliferation at 37ºC (Figure 7). By contrast, when we replaced Thr302 with
333 Val – an amino acid with properties similar to Thr, including a short sidechain – we saw rescue by
334 Gdm (Figure 7). We interpret these data as evidence that Gdm binds to ScCdc3 near Thr302 (or
335 Val302) in order to promote homodimerization, but does so in a way that is not recapitulated by an
336 Arg sidechain. Instead, Arg302 blocks functional Gdm binding. We conclude that the T302R
337 substitution alone cannot "reverse evolution", yet GdnHCl does. How?
338
339 **Gdm at ScCdc3 position 302 likely "tunes" a key His residue within the G homodimer**
340 **interface**

341 ScCdc3 Thr302 is predicted to lie within the septin α4 helix, which is located near both the nucleotide
342 binding pocket and the G interface (Figure 4). To begin to understand the molecular mechanism by
343 which Gdm at this position promotes Cdc3 homodimerization, we first examined 13 available septin
344 crystal structures and asked which other residues are nearby the residue in the position equivalent
345 to Thr302. The only non-α4-helix residue within 5 Å in every structure was a highly conserved His
346 (Table 1) residing in a loop at the end of the β4 strand previously dubbed the "*trans* loop 1" (Weirich,
347 Erzberger, & Barral, 2008), the same His predicted by our *in silico* modeling to contact bound Gdm
348 in Cdc3 (Figure 4A). In SEPT2•GppNHp, His158 contacts a highly conserved Asp within the Switch
349 II loop of the other protomer (Figure 4B) (Sirajuddin et al., 2009). By contrast, in the sole
350 *Chlamydomonas reinhardtii* septin, CrSEPT, (Pinto et al., 2017) or in human SEPT9•GTPγS, the
351 *trans* loop 1 His instead contacts the nucleotide bound by the other protomer (Figure 4B). Thus,
352 depending on which septins are involved, this key His residue makes either of two distinct contacts
353 across the septin G dimer interface. If during hetero-oligomerization two alternative septins (e.g.
354 Cdc3 or a mutant Cdc10) present to Cdc3 "competing" G interfaces in distinct conformations, then
355 the position of the *trans* loop 1 His may dictate which is ultimately chosen for incorporation, and
356 Gdm could influence this choice.

Table 1. Residues in close proximity to the positions corresponding to ScCdc3 Thr302 or His262 for other septins with solved crystal structures.

PDB entry, Septin•nucleotide (oligomeric state)	***Residues within 5Å (capitalized) of position corresponding to ScCdc3 Thr302****	***Residues within 5Å (capitalized) of His corresponding to ScCdc3 His262***
2QNR, HsSEPT2•GDP (G dimer)	*trans* loop 1 (pfg**H**Glkp)	α4 (reRLkk**R**ildE)
2QA5, HsSEPT2•GDP (G dimer)	*trans* loop 1 (pfg**H**glkp)	α4 (rerLkk**R**ilde)
3FTQ, HsSEPT2•GppNHp (G dimer)	*trans* loop 1 (pfg**H**Glkp)	α4 (rerLkk**R**ildE), Switch I (kieRtvq)**, Switch II (dtpgygDain)**
4Z51, HsSEPT3•GppNHp (monomer)	*trans* loop 1 (ptG**H**Slrp)	α4 (kseFkq**R**vrkE)
3SOP, HsSEPT3•GDP (G dimer)	*trans* loop 1 (ptG**H**Slrp)	α4 (kseFkq**R**vrke), P-loop (gqSGlgk)**, Switch I (vIPKtve)**
4Z54, HsSEPT3•GDP (G dimer)	*trans* loop 1 (ptG**H**Slrp)	α4 (kseFkq**R**vrkE), P-loop (gqSGlgk)**, Switch I (eeKIPKtve)**
3T5D, HsSEPT7•GDP (G dimer)	*trans* loop 1 (psg**H**Glkp)	α4 (qqFkk**Q**im), P-loop (geSGlgk)**
3TW4, HsSEPT7•GDP (G dimer)	*trans* loop 1 (psg**H**GLkp)	α4 (qqFkk**Q**im), P-loop (geSGlgk)**
5CYO, HsSEPT9•GDP (G dimer)	*trans* loop 1 (atG**H**Slrp)	α4 (rvhFkq**R**Itad), P-loop (gqSGlgk)**, Switch I (eeRIPKtie)**
5CYP, HsSEPT9•GTPγS (G dimer)	*trans* loop 1 (atg**H**SLrp)	α4 (rvhFkq**R**Itad), P-loop (gqsGlgk)**, Switch I (eeRIPKtie)**
4KV9, SmSEPT10•GDP (G dimer)	*trans* loop 1 (ptG**H**Slks)	α4 (lqkFka**R**ilse), P-loop (geTGigk)**
4KVA, SmSEPT10•GTP (G dimer)	*trans* loop 1 (ptG**H**Slks)	α4 (lqkFka**R**ilse), P-loop (geTgigk)**
5AR1, ScCdc11•empty (quasi-G dimer)***	*trans* loop 1 (ptg**H**Glke)	α4 (lklnkk**L**imeD)

* Residues at positions corresponding to ScCdc3 Thr302 were identified based on structure-guided alignments. SEPT2, Arg198; SEPT3, Arg224; SEPT7, Gln210; SEPT9, Arg442; SEPT10, Arg199; Cdc11, Leu187.
** Residues from the other protomer across the G interface.
***Dimer in solution is mediated by the C-terminal extension, and is unaffected by G interface mutations, thus contacts across the G interface are presumably crystal-induced.

357

358 In SEPT2•GppNHp, His158 is positioned in *cis* by contacts (~3 Å) with a Glu residue (Glu202)
359 (Sirajuddin et al., 2009), which lies one turn away from Arg198 in the α4 helix (Figure 4B). The Gdm
360 moeity of SEPT2 Arg198 (residue corresponding to Thr302 in Cdc3) is also within ~3 Å of the

361 backbone amide carbonyl of His158 (Figure 4B, Table 1), and thus is equally well located to position
362 His158. In CrSEPT and SEPT9•GTPγS, the Arg198 equivalent instead contacts the Glu202
363 equivalent (Figure 4B). Thus in some but not all septins the Gdm moiety of the α4 Arg is ideally
364 positioned to contact the *trans* loop 1 His and thereby potentially bias partner choice during septin
365 G dimerization. By contacting His262, Gdm bound near Thr302 in Cdc3 could bias Cdc3 towards
366 homodimerization and away from heterodimerization with Cdc10.
367
368 To look for additional evidence in support of this model, we next asked which other residues are
369 located in the vicinity (≤5 Å) of the *trans* loop 1 His in 13 available septin crystal structures. The α4
370 helix was the only region to meet this criterion in every structure, and, as expected, when Arg was
371 present at the position corresponding to ScCdc3 Thr302, it was always within 5 Å (Table 1). Apart
372 from the α4 helix, the Switch II loop, and adjacent *trans* loop 1 residues, residues within 5 Å of the
373 His fell within only two other regions: the P-loop and the Switch I loop (Table 1). These are precisely
374 the regions wherein we found non-conservative G interface substitutions between fungal species
375 that tolerate *CDC10* deletion and those that do not (Figure 4B). These observations provide strong
376 support for the idea that Gdm binding between the ScCdc3 α4 helix and His262 mimics an ancestral
377 evolutionary state and favors interaction with other similarly disposed Cdc3 molecules.
378
379 **The GTPase properties of the Cdc3 subunit dictate septin subunit composition**
380 Our data support a model in which Gdm influences whether or not septin complexes incorporate a
381 central homodimer of mutant Cdc10 molecules by influencing whether the Cdc3 *trans* loop 1
382 contacts the Switch II loop of another Cdc3 molecule, or points toward the site where nucleotide is
383 normally bound by Cdc10. This model is reminiscent of the conclusions of a previous study, in which
384 we proposed that the conformation of the Switch II loop in Cdc12 biases choice of its G-dimer
385 partner (Cdc11 or Shs1)(A. D. Weems & McMurray, 2017). In that study, we showed that a Switch

386 II mutation in Cdc12 is sufficient to bias partner choice. In an independent study (A. D. Weems et
387 al., 2014), we found that a spontaneous mutation (D210G) in the equivalent Switch II residue in
388 Cdc3 restores the ability of Cdc3 to interact with a nucleotide-free mutant Cdc10 at high
389 temperatures. Like Gdm, the *cdc3(D210G)* mutation rescues the TS phenotype of *cdc10(D182N)*
390 cells, but unlike Gdm it does so by restoring, rather than bypassing, incorporation of the mutant
391 Cdc10 subunits; in other words, the Switch II mutation D210G biases Cdc3 partner choice towards
392 nucleotide-free Cdc10, whereas Gdm biases partner choice away from it. Our model predicts that
393 in *cdc3(D210G)* cells Gdm should be less able to exclude the mutant Cdc10 than in cells expressing
394 WT Cdc3, because the mutant Cdc3 Switch II will be unable to accomplish the molecular contact(s)
395 with the Cdc3 *trans* loop 1 that Gdm promotes. Indeed, Gdm slightly reduced, but did not eliminate,
396 Cdc10(D182N)-GFP localization to septin rings in *cdc3(D210G)* cells (Figure 8A). These data are
397 consistent with an important role for contacts between the Switch II loop and the *trans* loop 1 during
398 Cdc3 homodimerization promoted by Gdm.
399
400 Since Cdc12 is an active GTPase, and the Switch II changes conformation upon GTP hydrolysis,
401 we interpreted our previous results with Switch II-mutant Cdc12 as evidence that the Switch II
402 conformation normally "communicates" across the G interface the phosphorylation state of Cdc12's
403 bound nucleotide (A. D. Weems & McMurray, 2017). We further bolstered this argument by mutating
404 in Cdc12 a Thr residue in the Switch I loop that is required for septin GTPase activity (Sirajuddin et
405 al., 2009; A. D. Weems & McMurray, 2017). Notably, Cdc3 lacks Thr in this position. How could
406 Gdm operate via Switch II conformation on Cdc3, a "dead" GTPase? We noticed in our phylogenetic
407 analysis of Cdc3 homologs in other fungal species that many possess the "catalytic Thr" (Figure 4–
408 figure supplement 1). In fact, there was a perfect correlation between the presence of the catalytic
409 Thr (or Ser) and the α4 Arg whose Gdm group is presumably mimicked by Gdm in Cdc3 (Figure 4–
410 figure supplement 1). Analogous to our model of Cdc12 G-partner choice via slow GTP hydrolysis

411 (A. D. Weems & McMurray, 2017), we reasoned that in a species with an active “Cdc3” GTPase, a
412 transient “Cdc3”•GTP molecule might prefer to dimerize with “Cdc10” in that species, and
413 “Cdc3”•GDP might prefer to form a homodimer, bypassing “Cdc10” incorporation into septin
414 complexes.
415
416 According to this model, because *Saccharomyces*, *Ashbya*, and *Kluyveromyces* species express
417 catalytically dead Cdc3 molecules, only Cdc3•GTP exists in these cells, and only Cdc10-containing
418 hetero-octamers are made. In *Aspergillus nidulans*, on the other hand, the Cdc3 homolog, AspB,
419 possesses the catalytic Thr (Figure 4–figure supplement 1, Figure 8–figure supplement 1), and this
420 species is known to produce a mix of octamers containing AspD (the Cdc10 homolog) and AspD-
421 less hexamers (Hernández-Rodríguez et al., 2014). We replaced the GTPase domain of ScCdc3
422 (residues 95-341) with that of AspB (residues 6-234; Figure 8–figure supplement 1) and assessed
423 Cdc10 incorporation into complexes by measuring the ratio of Cdc10-mCherry to Shs1-GFP in
424 septin rings of living cells. Consistent with our model, Cdc10-mCherry incorporation was markedly
425 reduced compared to cells with WT Cdc3 (Figure 8B), indicating that the GTPase properties of AspB
426 were sufficient to confer *Aspergillus*-like pathways of septin hetero-oligomer assembly, i.e., frequent
427 bypass of Cdc10 incorporation.
428
429 *S. cerevisiae* cells expressing the Cdc3-AspB chimera as the only source of Cdc3 were unable to
430 proliferate at 37ºC (Figure 8C). We hypothesized that this defect reflects misfolding at high
431 temperature of the Cdc3-AspB chimera to a conformation incapable of interacting with itself or with
432 Cdc10, and searched for spontaneous suppressors of the TS phenotype. We obtained a suppressor
433 in which proliferation at 37ºC was restored (Figure 8C). Sequencing the coding region of Cdc10
434 revealed a single nucleotide change causing the amino acid substitution Q265H (Figure 8D); the
435 Cdc3-AspB chimera was unchanged. In most septin structures, His in this position makes a critical

436 contact across the G interface with a highly conserved Trp residue in the "Sep4" motif (Pan et al.,
437 2007) (Figure 8E), the same Trp we mutated in the *cdc3(W364A)* mutant (see Figure 2D). Since
438 Gln replaces His here in ScCdc10 (and in the other fungal species with putatively GTPase-dead
439 Cdc3 homologs; Table 2), the Cdc3•GTP–Cdc10•GDP interface must involve a different kind of
440 interaction. We interpret these findings as evidence that stable association of Cdc10•GDP with
441 GDP-bound Cdc3-AspB, rather than the Cdc3•GTP with which Cdc10 co-evolved, requires His–Trp
442 contacts between Sep4 motifs of the sort found in other dimers between two GDP-bound septins.
443 Indeed, incorporation of Cdc10-mCherry into septin rings was partially restored in *cdc3-aspB*
444 *cdc10(Q265H)* cells (Figure 8B). Finally, Gdm was unable to fully rescue the TS phenotype of the
445 *cdc3-aspB CDC10*$^{+}$ strain (Figure 8C), as expected if the site of Gdm action is occluded by the α4
446 Arg present in the Cdc3-AspB chimera. These data provide further support for the idea that during
447 evolution ScCdc3 lost the ability to hydrolyze GTP to GDP and, consequently, the option of
448 assembling septin complexes without a central Cdc10 homodimer.
449

Table 2. Co-variation among fungal species of the "catalytic Thr" in Cdc3 homologs and His in the Cdc10 *trans* loop 1.

Species	***Amino acid at position corresponding to ScCdc3 Lys181***	***Amino acid at position corresponding to ScCdc10 Lys155***	***Amino acid at position corresponding to ScCdc10 Gln265***
S. cerevisiae	Lys	Lys	Gln
A. gossypii	Lys	Lys	Gln
K. lactis	Lys	Lys	Gln
C. albicans	Ser	Gln	Gln
A. nidulans	Thr	His	His
C. cinerea	Thr	His	His
U. maydis	Thr	His	His
N. crassa	Thr	His	His
M. oryzae	Thr	His	His
F. graminearum	Thr	His	His
C. neoformans	Thr	His	His
S. pombe	Thr	His	His

450 The GTPase domains of Cdc3 and AspB are <50% identical, and differ at many more positions than
451 the five identified by our phylogenetic analysis as co-varying with the α4 Arg and the catalytic Thr
452 (Figure 8–figure supplement 1). To ask if those five differences are sufficient to direct Cdc10 bypass

453 during septin assembly, we used CRISPR-Cas9 to cut the endogenous *CDC3* coding sequence
454 and, via homologous recombination, replace most of it with a "recoded" gene encoding the same
455 polypeptide sequence but using numerous synonymous codons, or with a similarly "recoded" gene
456 additionally encoding the five substitutions (P127E D128S K181T T302R Q306D). Recoding
457 allowed us to obtain transformants in which recombination occurred at the ends of our donor
458 templates, rather than in sequences immediately flanking the cut site, thus promoting incorporation
459 of all five substitutions. We also obtained a transformant in which only two substitutions were
460 incorporated, T302R Q306D, and we included this strain in our subsequent analysis. The recoded
461 control strain and the *P127E D128S K181T T302R Q306D* and *T302R Q306D* mutant strains were
462 indistinguishable from the parental *CDC3*$^{+}$ strain in terms of growth at all tested temperatures, and
463 also with regard to the relative amounts of Cdc10-mCherry incorporated into septin rings (Figure 8–
464 figure supplement 2). Thus, although we cannot rule out the possibility that recoding with
465 synonymous codons alters Cdc3 co-translational folding in some way that masks effects of the
466 amino acid changes we introduced, it appears that additional sequence changes are needed to
467 "reverse evolution" and restore the ability of Cdc3 to homodimerize robustly *in vivo*.
468

469 DISCUSSION

470 **Septin G dimer partner selection by "tuning" the *trans* loop 1 His via α4 Arg or Gdm**

471 We propose that Gdm binding adjacent to ScCdc3 Thr302 provides molecular contacts that position
472 His262 to interact in *trans* with an Asp residue from a septin Switch II loop in a "GTP state", such
473 as that provided by another Cdc3•GTP. The spontaneous mutation we previously found to promote
474 Cdc3 homodimerization (McMurray et al., 2011) alters a *trans* loop 1 residue immediately adjacent
475 to Cdc3 His262, Gly261. Val in this position probably also "tunes" the configuration of His262 to
476 favor Cdc3 homodimerization via interaction with Cdc3 Asp201. Specific configurations of the
477 Switch II loop clearly dictate G dimer partner choice, as mutating the residue corresponding to Cdc3

478 Asp210 promotes both stable Cdc3 heterodimerization with nucleotide-free Cdc10 (A. D. Weems et
479 al., 2014) and biased selection of Shs1 by Cdc12 (A. D. Weems & McMurray, 2017). Mutating a
480 nearby Asp in the Switch II loop of human SEPT7 also allows homodimerization when only a non-
481 hydrolyzable GTP analog is available (Zent & Wittinghofer, 2014). "Tuning" by Gdm via *cis*
482 interactions presumably occurs prior to G dimerization, and is likely a transient event: once the *trans*
483 loop 1 His has engaged either the Switch II Asp or nucleotide (or nearby where nucleotide normally
484 binds, in the case of nucleotide-free mutant Cdc10), the Arg–His interaction probably need not
485 persist post-dimerization. It follows that Gdm may not remain bound to Cdc3 following G
486 dimerization, and thus falls under a broad definition of a "pharmacological" or "chemical" chaperone.
487

488 Since in otherwise WT cells Gdm promotes bypass of mutant Cdc10 molecules with substitutions
489 in various locations in the G interface and nucleotide-binding pocket, but not WT Cdc10, additional
490 contacts between WT Cdc10•GDP and Cdc3•GTP likely favor Cdc3–Cdc10 heterodimerization over
491 Cdc3 homodimerization despite the presence of Gdm. Poorer GdnHCl rescue of *cdc10(G44D)* (P-
492 loop mutant) relative to *cdc10(D182N)* (G4 mutant) and *cdc10(G100E)* (Switch II mutant) may
493 reflect a comparatively better ability of Cdc10(G44D) molecules to, despite temperature-induced
494 misfolding, occupy the Cdc3 G interface and resist exclusion, thereby interfering with hexamer
495 assembly. Bound nucleotide itself may provide the key contacts that distinguish WT Cdc10 from the
496 mutants, with Cdc10(G44D) subunits being more successful than the other mutants at binding
497 nucleotide. At moderate temperatures (22-27ºC) Cdc3 molecules carrying the G365R substitution
498 are slow to acquire the conformation competent for interaction with Cdc10 (Schaefer, Heasley,
499 Odde, & McMurray, 2016). Our observation that GdnHCl exacerbated the TS phenotypes of
500 *cdc3(G365R)* cells (Figure 1A) thus provides further evidence of a bias imposed by Gdm on Cdc3
501 toward conformations that are suboptimal for interaction with Cdc10, the effects of which are

502 masked in WT cells but become obvious when combined with additional folding biases like the
503 G365R substitution.
504
505 Whereas Gdm was unable to drive Cdc10 bypass in WT cells, swapping the GTPase domain of
506 Cdc3 for that of AspB was sufficient to promote bypass of WT Cdc10 (Figure 8B), consistent with
507 the idea that Cdc3•Gdm only partially mimics the ancestral homodimer configuration. Finally,
508 introducing into Cdc3 the five residues (including the catalytic Thr and α4 Arg) that are found in
509 Cdc3 homologs in species that tolerate loss of the Cdc10 homolog was unable to drive exclusion of
510 Cdc10 from septin complexes (Figure 8–figure supplement 2). Cdc12 natively possesses four of
511 these five residues (Figure 8–figure supplement 1), yet forcing septin hexamer assembly via non-
512 native Cdc12 homodimers (by deleting *SHS1* and *CDC11*) results in *S. cerevisiae* cells that, like
513 *cdc10*Δ, cannot proliferate at 37ºC (McMurray et al., 2011). Clearly GTPase activity and the
514 presence of these residues is insufficient for robust septin homodimerization, and additional
515 changes are likely key.
516
517 **Insights into major events during septin evolution**
518 Although septins are absent from land plants, protein transport across the outer envelope
519 membrane of chloroplasts is mediated by TOC complexes containing a small GTPase subunit,
520 Toc34, that shares high structural homology to septins. Others have noted (Weirich et al., 2008)
521 that the septin *trans* loop 1 is in a similar position to a Toc34 interface loop that makes key contacts
522 with nucleotide bound by the partner protein across a homodimer interface (Figure 9A). In both pea
523 (*Pisum sativum*) and *Arabidopsis thaliana* an Arg residue in the Toc α4 helix projects towards the
524 homodimer interface, to within 5 Å of the *trans* loop 1 equivalent (Figure 9A). Arg in this position is
525 conserved among all Toc34 homologs (Figure 9B). We conclude that Arg-mediated α4 helix tuning

526 of the *trans* loop 1 for specific dimerization events across the nucleotide-binding-pocket-containing
527 interface is an evolutionarily ancient mechanism that predated the appearance of septins *per se*.
528
529 Following loss of the α4 Arg in the fungal lineage giving rise to *S. cerevisiae*, *A. gossypii*, and *K.*
530 *lactis*, the amino acid at the position equivalent to ScCdc3 Thr302 diverged rapidly. Ser or Ala
531 appear in its place in other species within the genus *Saccharomyces*, which share >86% sequence
532 identity with ScCdc3 (Figure 9C). By comparison, within the genus *Candida* Arg is invariant among
533 six species sharing as little as 35% identity with *C. albicans* Cdc3 (Figure 9C). These observations
534 are consistent with the notion that Thr in this position does not make specific structural contributions
535 to septin assembly.
536
537 One clear prediction from this model is that in the two fungal lineages distinguished by the presence
538 or absence of the Cdc3 "catalytic" Thr, the Cdc10 subunit should have evolved differently, to
539 recognize in one case only Cdc3•GTP and, in the other, either Cdc3•GTP and Cdc3•GDP. Our
540 unbiased identification of the *cdc10(Q265H)* mutation in cells expressing the Cdc3-AspB chimera
541 provided one example of how Cdc10 adapted to interacting with a Cdc3 subunit "fixed" in the GTP-
542 bound state. Others previously noted (Sirajuddin et al., 2009) that ScCdc10 is unusual among
543 septins in that it has Lys rather than His in the *trans* loop 1. If the residue in this position acts to
544 promote interaction with a G dimer partner in a specific nucleotide state, this may explain why Lys
545 in this position is shared by AgCdc10 and KlCdc10, but not any of the Cdc10 homologs in the fungal
546 species in which the Cdc3 homolog retains the "catalytic Thr" (Table 2). Co-variation of these
547 residues likely reflects co-evolution. Figure 9–figure supplement 1A illustrates a possible pathway
548 of such changes during septin evolution.
549
550 Were Cdc10-less hexamers specifically selected against during evolution of a fungal lineage?
551 Compared to other closely-related fungi, *Ashbya*, *Kluyveromyces*, and *Saccharomyces* share little

552 in common with regard to the cellular functions in which septins are known to operate, such as
553 polarity, morphogenesis, cytokinesis, or sporulation. Hence it is hard to imagine how losing septin
554 hexamers could provide a specific selective advantage to a common ancestor, though this may
555 reflect our incomplete understanding of what septin hexamers do differently than septin octamers.
556 On the other hand, the assembly of hexamers liberates the Cdc10 subunits to act elsewhere, and
557 specific functions of "free" Cdc10 homologs could represent an evolutionary pressure point to
558 maintain GTPase activity in Cdc3 homologs. Indeed, in *U. maydis* (Alvarez-Tabarés & Pérez-Martín,
559 2010) and *A. nidulans* (Hernández-Rodríguez et al., 2014) the Cdc10 homologs are found in distinct
560 cellular structures independently of the other septins, where they may function independently, as
561 well.
562
563 Many human cell types also natively produce both septin hexamers and octamers (Abbey et al.,
564 2016; Kim, Froese, Estey, & Trimble, 2011; Sellin, Holmfeldt, Stenmark, & Gullberg, 2011; Sellin,
565 Sandblad, Stenmark, & Gullberg, 2011; Sellin, Stenmark, & Gullberg, 2014). Incorporation of a
566 subunit from the SEPT3 group (SEPT3, SEPT9, or SEPT12) appears to confer functions to human
567 octamers that hexamers lack, such as microtubule bundling (Bai et al., 2013), vesicle trafficking in
568 neurons (Karasmanis et al., 2018), directing proper spermatogenesis (Kuo et al., 2015), and
569 membrane abscission at the end of cytokinesis (Estey, Ciano-Oliveira, Froese, Bejide, & Trimble,
570 2010). Human and yeast septin octamers were thought to differ in where within the complex the
571 "extra" subunits incorporate, with SEPT3-group septins like SEPT9 occupying the "terminal"
572 positions at both octamer ends (Kim et al., 2011). However, two recent reports (Mendonça et al.,
573 2019; Soroor et al., 2019) suggest that in fact SEPT3-group septins form a central homodimer
574 flanked by SEPT7, with SEPT6 and SEPT2 occupying the penultimate and terminal positions,
575 respectively. In this "revised" organization, the GTPase-dead subunit position (the SEPT6 group)
576 corresponds to that of Cdc12, and the Cdc3 position is occupied by SEPT7, an active GTPase (see
577 Figure 9–figure supplement 1B). Notably, a mutation (S63N) that doubles SEPT7 GTPase activity

578 in vitro shifts assembly in vivo from primarily hetero-octamers to smaller complexes (Abbey et al.,
579 2016), consistent with our model that septins in the GDP-bound state are prone to homodimerization
580 across the G interface and exclusion of intervening subunits.
581
582 Cdc10 and SEPT9 fall into one ancient evolutionary clade, whereas Cdc3, Cdc12, SEPT6 and
583 SEPT7 all appear to have distinct origins (Auxier et al., 2019). Thus the loss of septin GTPase
584 activity occurred multiple times independently. By demonstrating that GTPase activity facilitates
585 promiscuity during dimerization, and thereby expands the repertoire of septin hetero-oligomers, our
586 findings provide the first molecular rationale for the evolution of GTPase-dead septins: to narrow
587 the variety of building blocks available for higher-order assemblies. A similar logic may explain the
588 most famous example of loss of GTPase activity of a cytoskeletal protein, that of the α subunit of
589 the tubulin heterodimer.
590
591 **Chemical rescue by guanidine hydrochloride *in vivo***
592 The ability of Gdm to occupy vacancies created by the mutation of Arg residues is well documented
593 *in vitro* for a wide variety of enzymes (Baldwin et al., 1998; Barnett, Amyes, Wood, Gerlt, & Richard,
594 2010; Boehlein, Walworth, Richards, & Schuster, 1997; Dugdale et al., 2010; Goedl & Nidetzky,
595 2008; Guillén Schlippe & Hedstrom, 2005; Hung et al., 2014; Lehoux & Mitra, 2000; Phillips et al.,
596 1992; Rynkiewicz & Seaton, 1996), but effects of GdnHCl on living cells were limited to Gdm binding
597 at sites in WT proteins or nucleic acids: in the ATP-binding pocket of Hsp104 and its relatives
598 (Zeymer, Werbeck, Schlichting, & Reinstein, 2013), in the intracellular pore of voltage-gated
599 potassium channels (Kalia & Swartz, 2011), in the enteroviral 2C protein (Sadeghipour, Bek, &
600 McMinn, 2012), and, most recently, in bacterial riboswitches that sense intracellular Gdm and
601 induce a cellular response to detoxify it (Nelson, Atilho, Sherlock, Stockbridge, & Breaker, 2017).
602 The function of a rationally-designed Arg-mutant kinase can be rescued *in vitro* by GdnHCl
603 (Williams, Wang, & Cole, 2000), and the same mutant is rescued by imidazole *in vivo* (Qiao, Molina,

604 Pandey, Zhang, & Cole, 2006), but our findings that GdnHCl can functionally replace an Arg in Cdc3
605 represent the first documented case of "chemical rescue" by GdnHCl *in vivo*.
606
607 The apparent requirement for GdnHCl to be present during Cdc3 folding illustrates how our case of
608 GdnHCl mimicry of a "missing" Arg sidechain is fundamentally distinct from the other examples of
609 "chemical rescue" by GdnHCl, in which a protein that had evolved to adopt a specific conformation
610 was mutated at a single site in order to perturb this conformation (or, in most cases, interaction with
611 a substrate molecule), and Gdm was able to restore the native fold or interaction. In those prior
612 studies, the mutated protein was already near the native conformation and only a small effect of
613 GdnHCl was required to achieve that conformation. In our case, a WT protein that had evolved to
614 avoid a particular conformation was induced to reach that non-native conformation only when
615 GdnHCl was present during its folding. During Cdc3 folding in the absence of Gdm, other
616 intramolecular interactions drive acquisition of the low-energy native conformation that disfavors
617 homodimerization. Gdm would have to act early, in a manner equivalent to how canonical
618 chaperones direct the folding pathways of their clients. The ability of the T302R mutation to block,
619 but not to mimic, the effect of GdnHCl could be explained by an ability of Gdm to make
620 intramolecular contacts within Cdc3 that, because it is tethered to the polypeptide backbone, the
621 Gdm moiety of an Arg sidechain cannot. Our findings do not exclude the possibility that additional
622 Gdm molecules bind elsewhere in Cdc3 and contribute to Cdc3 folding, with occupancy of the site
623 near Thr302 being necessary but not sufficient.
624
625 In yeast cells cultured in 1 mM GdnHCl the intracellular concentration is ~20 mM (Jones, Song, &
626 Masison, 2003). Thus in the conditions in we observed *cdc10* rescue Gdm likely binds to hundreds
627 or thousands of proteins, with few adverse effects. Indeed, GdnHCl is approved by the Food and
628 Drug Administration of the USA for use in humans, and at low doses has few serious side effects

629 (S. J. Oh, Kim, Head, & Claussen, 1997). Exploiting the ability of Gdm to replace Arg in living cells
630 represents a compelling area for future research, particularly as a possible therapeutic
631 “pharmacoperone” (Conn et al., 2014). Finally, given the evidence that bacteria evolved ways to
632 manage intracellular Gdm (including actively exporting it (Kermani, Macdonald, Gundepudi, &
633 Stockbridge, 2018)), Gdm may, like the naturally occurring osmolyte trimethylamine N-oxide
634 (Bandyopadhyay et al., 2012) and the chaperone Hsp90 (Lindquist, 2009), influence evolution by
635 buffering against the phenotypic consequences of mutations.
636

637 MATERIALS AND METHODS

638 **Fungal strains and plasmids**

639 The sources and genotypes for all fungal strains and plasmids are listed in the Supporting
640 Information (S1 Table). Primer and synthetic gene sequences are listed in S2 Table. Yeast were
641 transformed using the Frozen-EZ Yeast Transformation II Kit (Zymo Research). Genetic
642 manipulations were otherwise performed according to standard methods (Amberg, Burke, &
643 Strathern, 2005), except for the creation of the *cdc3-aspB* chimera and the *CDC3(P127E D128S*
644 *K181T T302R Q306D)* and *CDC3(T302R Q306D)* strains and associated "recoded" control strain,
645 which were made in yeast strain JTY5397 using CRISPR-Cas9 cleavage of the *CDC3* locus and
646 repair with PCR products as donor templates, following an established protocol (Akhmetov et al.,
647 2018) and using plasmid pEM-CDC3-CRISPR1, a gift of Ed Marcotte, which encodes Cas9 and a
648 guide RNA targeting nucleotides 1039-1069 of the *CDC3* ORF (5' GATATTGTAGAGAACTACAG
649 3'). To create the donor template for the *cdc3-aspB* chimera, a portion of the *aspB* coding sequence,
650 the *aspB* plasmid pRL10, which was a gift of Michelle Momany and is based on the yeast two-hybrid
651 vector pGBKT7 (Takara Bio/Clontech), was used as template for a PCR reaction with Q5
652 polymerase (New England Biolabs) and primers Cdc3AspBfw and Cdc3AspBextend1 according to
653 the polymerase manufacturer's instructions. The resulting product, which included the sequence
654 encoding part of AspB flanked by *CDC3* sequences, was used as template for a second Q5 reaction
655 with primers Cdc3AspBfw and Cdc3GTPase_extend2, in order to extend the *CDC3* homology to
656 span the site of the Cas9 cut. To create the donor template for the *CDC3(P127E D128S K181T*
657 *T302R Q306D)* strain and its "recoded" control, an 870-nucleotide segment of the Cdc3 ORF
658 corresponding to the GTPase domain was synthesized (Integrated DNA Technologies) with multiple
659 synonymous codons replacing the native sequence (S2 Table), representing 67 nucleotide changes
660 but no amino acid substitutions. An otherwise identical sequence also including the *P127E D128S*
661 *K181T T302R Q306D* mutations was also synthesized (S2 Table). Donor template PCRs were done

662 with Q5 and primers G1KTTRQDfw and Cdc3recodere (S2 Table). Transformants were screened
663 by PCR of the *CDC3* locus and subsequent sequencing. Low-copy, *LEU2*-marked *CDC3* or *CDC3-*
664 *GFP* plasmids were pFM831 (Sirajuddin et al., 2009) or pML109 (Nagaraj et al., 2008). Plasmids
665 YCpHLcdc3(T302R)-GFP and YCpHLcdc3(T302V)-GFP were made via site-directed mutagenesis
666 using template plasmid pML109 by Keyclone Technologies (San Marcos, CA). Low-copy, *kanMX-*
667 marked plasmid YCpK-Cdc10-1-GFP, encoding *cdc10(D182N)-GFP*, was described previously
668 (Johnson et al., 2015).
669
670 **Media and additives**
671 *S. cerevisiae* media: Rich growth medium was YPD (1% yeast extract (#Y20020, Research
672 Products International Corp., Mount Prospect, IL), 2% peptone (#P20241, RPI Corp.), 2% dextrose
673 (#G32045, RPI Corp.)). Synthetic growth medium was based on YC (0.1 g/L Arg, Leu, Lys, Thr, Trp
674 and uracil; 0.05 g/L Asp, His, Ile, Met, Phe, Pro, Ser, Tyr and Val; 0.01 g/L adenine; 1.7 g/L Yeast
675 Nitrogen Base (YNB) without amino acids or ammonium sulfate; 5 g/L ammonium sulfate; 2%
676 dextrose) with individual components (from Sigma Aldrich, St. Louis, MO, or RPI Corp.) eliminated
677 as appropriate for plasmid selection. For solid media, agar (#A20030, RPI Corp.) was added to 2%.
678 For counterselection against *URA3*, 5-fluoro-orotic acid monohydrate (#F5050, United States
679 Biological, Salem, MA) was added to modified YC medium (1 g/L Pro in place of ammonium sulfate,
680 0.02 g/L uracil) to final 0.6 g/L. For counterselection against *LYS2*, α-aminoadipate (#A1374-09, US
681 Biological) at 2 g/L replaced ammonium sulfate in YC medium containing only YNB, uracil, His, Leu,
682 Lys, Met, Trp, and dextrose. G418 sulfate (Geneticin®, #G1000, US Biological) was added to YPD
683 at 200 μg/mL for selection of *kanMX*.
684
685 *A. gossypii* media: Ashbya strains were grown in 10 mL Ashbya Full Medium (AFM, 1% casein
686 peptone, 1% yeast casein extract, 2% dextrose and 0.1% myo-inositol) containing ampicillin (100

687 μg/mL), CloNAT (50 μg/mL) and G-418 (200 μg/mL). For imaging, cells were washed into 2X low-
688 fluorescence minimal medium (per liter: 3.4 g YNB without amino acids or ammonium sulfate, 2 g
689 Asp, 2 g myo-inositol, 40 g dextrose, 20 mg adenine, 21 g 3-(N-morpholino)propanesulfonic acid
690 (MOPS), pH adjusted to 7.0 with sodium hydroxide).
691
692 GdnHCl (#G4505, Sigma Aldrich, St. Louis, MO), ArgHCl (#A5131, Sigma Aldrich), aminoguanidine
693 HCl (#sc-202931, Santa Cruz Biotechnology, Santa Cruz, CA) and N-ethylguanidine HCl (#sc-
694 269833, Santa Cruz Biotechnology) were dissolved in water.
695
696 **Growth curves**
697 Growth curves were generated using a Cytation 3 plate reader (BioTek, Winooski, Vermont) as
698 described previously (Schaefer et al., 2016) using a starting overnight culture of the *cdc10(D182N)*
699 strain CBY06417 grown at 22ºC prior to dilution into 200 µL YPD medium in each well.
700
701 **Immunofluorescence**
702 Immunofluoresence was performed as described previously (Pringle et al., 1989) using an anti-
703 Cdc11 primary antibody (#sc7170, Santa Cruz Biotechnology, Santa Cruz, CA) and Alexa-Fluor
704 488-labeled anti-rabbit secondary antibody (#20012, Biotium, Inc., Fremont, CA) at a 1:5000 and
705 1:1000 dilution, respectively.
706
707 **Bacterial esxpression and purification of septins**
708 BL21 Star™(DE3) *E. coli* cells (ThermoFisher Scientific # C601003) were transformed with plasmids
709 pMVB121 (encoding 6xHis-Cdc12) and pMVB133 (encoding untagged Cdc3 and Cdc11) and grown
710 overnight in 3 mL LB medium (per L: 10 g tryptone, 5 g yeast extract, 10 g NaCl) with ampicillin (50
711 µg/mL), chloramphenicol (34 µg/mL), and varying amounts of GdnHCl (from 0 mM to 96 mM) at

712 37ºC in glass culture tubes with agitation. Growth was assessed qualitatively and was equivalent
713 for all cultures, so 50 mM was chosen as the concentration for subsequent experiments. 1-L 2XTY
714 (per L: 16 g Tryptone, 10 g yeast extract, 5 g NaCl) cultures with ampicillin, chloramphenicol and
715 with or without 50 mM GdnHCl were grown at 37ºC with shaking to OD_{600} between 0.6 and 1.0, at
716 which point IPTG was added to 0.1 mM and the culture was incubated overnight. Cells were
717 collected by centrifugation, resuspended in a minimal volume of lysis buffer (300 mM NaCl, 2 mM
718 $MgCl_2$, 40 μM GTP, 1 mM EDTA, 5 mM β-mercaptoethanol, 0.5% Tween-20, 12% glycerol, 50 mM
719 Tris-HCl, pH 8.0, with or without 50 mM GdnHCl) and frozen by dripping into liquid nitrogen. Cells
720 were thawed in 30 mL lysis buffer containing protease inhibitors (Complete EDTA-free, Roche
721 #11836170001), lysozyme and benzonase (Sigma-Aldrich #E8263). Cells were sonicated for 5
722 minutes total (30 seconds on, 30 seconds off) with a tip sonicator. Lysates were clarified by
723 centrifugation at 12,000xg at 4ºC and mixed with 200 μL of a slurry of Ni^{2+}-NTA agarose (Qiagen
724 #30210) that had been equilibrated in lysis buffer. After rotating for 1 hour at 4ºC, beads were
725 collected by centrifugation, washed two times with 5 mL of 300 mM NaCl, 20 mM imidazole, 0.1%
726 Tween-20, and 50 mM Tris-HCl, pH 8.0, with or without 50 mM GdnHCl. The beads were poured
727 into a column and the septin complex was eluted in fractions from the beads with 500 mM NaCl, 40
728 μM GTP, 500 mM imidazole, 50 mM Tris-HCl, pH 8.0, with or without 50 mM GdnHCl. Aliquots of
729 fractions were analyzed by SDS-PAGE and Coomassie staining, and imidazole was removed from
730 the fraction containing the peak of septin complex via buffer exchange into 500 mM NaCl, 40 μM
731 GTP, 50 mM Tris-HCl, pH 8.0 using a PD-10 column (GE Healthcare LifeSciences # 17085101).
732 The sample was further purified by size exclusion chromatography using a Superdex 200 column
733 and 50 mM Tris-HCl, 300 mM NaCl pH 8, supplemented with or without 50 mM GnHCl). The
734 fractions were analyzed by SDS-PAGE and Coomassie staining to collect the final samples for
735 electron microscopy.
736
737 **Electron microscopy**

738 For EM of yeast cells, cells were cultured at 37°C in YPD medium with 3 mM GdnHCl and collected
739 by vacuum filtration, then vitrified by high pressure freezing using a HPM100 (Leica Microsystems,
740 Wetzlar, Germany) apparatus. The frozen cells were cryo-substituted using a Leica ASF2 device in
741 a medium containing osmium tetroxide (1%), water (5%) and uranyl acetate (0.1%) in acetone using
742 a protocol described elsewhere (Bertin & Nogales, 2016). The cells were embedded into Epon
743 before being sectioned into 50 nm sections using an ultramicrotome UC6 (Leica) equipped with a
744 4.5 mm diamond knife (Diatome, Hatfield, PA). The resulting sections were deposited onto copper
745 electron microscopy grids (mesh size of 100). The images were collected with a 120 kV Lab6
746 microscope (Technai Spirit, FEI, Eindhoven, Netherlands) equipped with a CCD Quemesa camera
747 (Olympus, Tokyo, Japan).
748
749 For EM of septin complexes purified from *E. coli*, 4 µL of sample at a final concentration of 0.01
750 mg/mL for high salt conditions or 0.1 mg/mL for low salt conditions were absorbed for 30 seconds
751 on a glow-discharged carbon coated grid (Electron Microscopy Sciences, ref CF300-CU). The grids
752 were then negatively stained for 1 minute using 2% uranyl formate. Data was collected using either
753 a Tecnai Spirit microscope (Thermofischer, FEI, Eindhoven, The Netherlands) operated at an
754 acceleration voltage of 80Kv and equipped with a Quemesa (Olympus) camera or with a Lab6 G2
755 Tecnai (ThermoFisher, FEI, Eindhoven, the Netherlands) operated at an acceleration voltage of 200
756 kV. The data was acquired using a 4k X 4k F416 CMOS camera (TVIPS) in an automated manner
757 using the EMTools software suite (TVIPS).
758
759 **Two dimensional image processing for single-particle EM images**
760 Square boxes were hand-picked from the images respectively using the boxer tool from the EMAN
761 software suite (Ludtke, Baldwin, & Chiu, 1999). 4233 boxes of 135 pixels were picked from the

762 control sample while 3247 boxes of 203 pixels were picked from images collected of the sample
763 grown in the presence of GdnHCl. Subsequent processing was carried out using SPIDER (Frank et
764 al., 1996). After normalization of the particles, a non-biased reference-free algorithm was used to
765 generate 20 classes. Multi-reference alignment followed by classification was carried out to
766 generate about 50 classes. Fast Fourier transform analysis and power spectrum generation were
767 performed in ImageJ (Schneider, Rasband, & Eliceiri, 2012).
768
769 **Fluorescence microscopy**
770 All images of *S. cerevisiae* were captured using an EVOSfl all-in-one microscope (Advanced
771 Microscopy Group, Mill Creek, Washington) using a 60X objective and Texas Red, RFP, or GFP
772 LED/filter cubes, as described previously (Johnson et al., 2015). Bud neck fluorescence was
773 quantified using line scans as described previously (Johnson et al., 2015; A. D. Weems & McMurray,
774 2017). Intensity values or ratios thereof were plotted using GraphPad Prism 8.0, using the medium
775 smoothing (kernel density) setting for violin plots. When necessary for presentation, images were
776 inverted and brightness- and contrast-adjusted using Adobe Photoshop (Adobe Systems
777 Incorporated, San Jose, California), always the same way for every image of the same type.
778
779 *Ashbya* cells in minimal low-fluorescence medium were mounted onto 2% agarose gel pads and
780 the edges were sealed with Valap (a 1:1:1 mixture of vaseline, lanolin, and paraffin). Images were
781 acquired using a Zeiss Axioimager-M1 upright light microscope (Carl Zeiss, Jenna, Germany)
782 equipped with a Plan-Apochromat 63X/1.4 numerical aperture oil objective and an Exfo X-Cite 120
783 lamp. Fluorescence imaging was performed using Zeiss 38HE filter cubes (GFP). Images were
784 acquired using an Orca-AG charge-coupled device (CCD) camera driven by μManager.
785
786 ***In silico* docking, structure prediction, and analysis**

787 Visualization and rendering of structures in PDB format was performed using MacPyMol
788 (Schrödinger, New York, NY). Residues within 5 Å of other residues were identified using the
789 "around" command. Structure prediction for ScCdc3 was performed using the I-TASSER server
790 (http://zhanglab.ccmb.med.umich.edu/I-TASSER/) (Zhang, 2008) and ScCdc3 sequence truncated
791 to amino acids 116-411 to match the template model, SEPT2•GppNHp (PDB 3FTQ). Molecular
792 docking was performed using a local installation of AutoDock Vina (Trott & Olson, 2010) via Chimera
793 1.11 (http://www.rbvi.ucsf.edu/chimera) (Pettersen et al., 2004), using a search volume containing
794 the entire "receptor" model.
795
796 **Sequence alignments**
797 Multiple alignments were performed using the COBALT tool at the NCBI server
798 (https://www.ncbi.nlm.nih.gov/tools/cobalt/) or, for sequences of yeast species not available via
799 NCBI, using the "Fungal Alignment" function at the Yeast Genome Database (*Saccharomyces*
800 *Genome Database*, n.d.). In some cases, sequences obtained via the Yeast Genome Database
801 were aligned with other sequences via COBALT.
802
803 **DNA sequencing**
804 Genomic DNA from the *cdc3-AspB* suppressor strain was isolated as described previously and used
805 as template in Q5 PCR reactions with primers 5'cdc3fw and 3'cdc3re, or 5'cdc10fw and 3'cdc10re
806 performed according to the polymerase manufacturer's instructions. Following treatment with
807 alkaline phosphatase and Exonuclease I (Thermo Scientific Fermentas), the purified PCR product
808 was directly sequenced at the sequencing facility of the Barbara Davis Center for Childhood Obesity,
809 with the same primers used for amplification and, for *CDC10*, with primer cdc10midfw. To confirm
810 correct strain construction, sequencing of other loci was performed in an equivalent manner with
811 appropriate primers (S2 Table).
812

813 **Choice of sample sizes and statistical analysis**

814 Sample sizes (*n*, number of cells) for fluorescence microscopy were chosen based on our ability to
815 detect decreases in bud neck localization in our previous studies (Johnson et al., 2015; A. D. Weems
816 & McMurray, 2017). Analysis of effect sizes and generation of effect size plots were performed using
817 DABEST (data analysis with bootstrap-coupled estimation) (Ho, Tumkaya, Aryal, Choi, & Claridge-
818 Chang, 2019) via the online server at http://www.estimationstats.com. Other violin plots were
819 generated with Prism 8.0 (Graphpad) using the "medium" smoothing/kernel density setting.

820

821 ACKNOWLEDGEMENTS

822 We thank Michelle Momany (University of Georgia, USA) for fruitful discussions about septin
823 evolution and sharing unpublished reagents. The UCSF Chimera software package is developed
824 by the Resource for Biocomputing, Visualization, and Informatics at the University of California, San
825 Francisco (supported by NIGMS P41-GM103311). We also acknowledge the PICT-IBiSA (Institut
826 Curie, Paris).

827

828 REFERENCES

829 Abbey, M., Hakim, C., Anand, R., Lafera, J., Schambach, A., Kispert, A., … Menon, M. B. (2016). GTPase
830 domain driven dimerization of SEPT7 is dispensable for the critical role of septins in fibroblast
831 cytokinesis. *Scientific Reports*, *6*, 20007. https://doi.org/10.1038/srep20007

832 Akhmetov, A., Laurent, J. M., Gollihar, J., Gardner, E. C., Garge, R. K., Ellington, A. D., … Marcotte, E. M.
833 (2018). Single-step Precision Genome Editing in Yeast Using CRISPR-Cas9. *Bio-Protocol*, *8*(6).
834 https://doi.org/10.21769/BioProtoc.2765

835 Alvarez-Tabarés, I., & Pérez-Martín, J. (2010). Septins from the phytopathogenic fungus Ustilago
836 maydis are required for proper morphogenesis but dispensable for virulence. *PloS One*, *5*(9),
837 e12933. https://doi.org/10.1371/journal.pone.0012933

838 Amberg, D., Burke, D., & Strathern, J. (2005). *Methods in Yeast Genetics: A Cold Spring Harbor*
839 *Laboratory Course Manual, 2005 Edition*. Cold Spring Harbor Laboratory Press.

840 An, H., Morrell, J. L., Jennings, J. L., Link, A. J., & Gould, K. L. (2004). Requirements of fission yeast
841 septins for complex formation, localization, and function. *Molecular Biology of the Cell*, *15*(12),
842 5551–5564. https://doi.org/10.1091/mbc.E04-07-0640

843 Auxier, B., Dee, J., Berbee, M. L., & Momany, M. (2019). Diversity of opisthokont septin proteins reveals
844 structural constraints and conserved motifs. *BMC Evolutionary Biology*, *19*(1), 4.
845 https://doi.org/10.1186/s12862-018-1297-8

846 Bai, X., Bowen, J. R., Knox, T. K., Zhou, K., Pendziwiat, M., Kuhlenbäumer, G., … Spiliotis, E. T. (2013).
847 Novel septin 9 repeat motifs altered in neuralgic amyotrophy bind and bundle microtubules.
848 *The Journal of Cell Biology*, *203*(6), 895–905. https://doi.org/10.1083/jcb.201308068

849 Baldwin, E., Baase, W. A., Zhang, X. j, Feher, V., & Matthews, B. W. (1998). Generation of ligand binding
850 sites in T4 lysozyme by deficiency-creating substitutions. *Journal of Molecular Biology*, *277*(2),
851 467–485.

852 Bandyopadhyay, A., Saxena, K., Kasturia, N., Dalal, V., Bhatt, N., Rajkumar, A., … Chakraborty, K. (2012).
853 Chemical chaperones assist intracellular folding to buffer mutational variations. *Nature*
854 *Chemical Biology*, *8*(3), 238–245. https://doi.org/10.1038/nchembio.768
855 Barnett, S. A., Amyes, T. L., Wood, B. M., Gerlt, J. A., & Richard, J. P. (2010). Activation of R235A mutant
856 orotidine 5'-monophosphate decarboxylase by the guanidinium cation: Effective molarity of
857 the cationic side chain of Arg-235. *Biochemistry*, *49*(5), 824–826.
858 https://doi.org/10.1021/bi902174q
859 Berepiki, A., & Read, N. D. (2013). Septins are important for cell polarity, septation and asexual spore
860 formation in Neurospora crassa and show different patterns of localisation at germ tube tips.
861 *PloS One*, *8*(5), e63843. https://doi.org/10.1371/journal.pone.0063843
862 Bertin, A., McMurray, M. A., Grob, P., Park, S.-S., Garcia, G., Patanwala, I., … Nogales, E. (2008).
863 Saccharomyces cerevisiae septins: Supramolecular organization of heterooligomers and the
864 mechanism of filament assembly. *Proceedings of the National Academy of Sciences of the United*
865 *States of America*, *105*(24), 8274–8279. https://doi.org/10.1073/pnas.0803330105
866 Bertin, A., & Nogales, E. (2016). Characterization of Septin Ultrastructure in Budding Yeast Using
867 Electron Tomography. *Methods in Molecular Biology (Clifton, N.J.)*, *1369*, 113–123.
868 https://doi.org/10.1007/978-1-4939-3145-3_9
869 Boehlein, S. K., Walworth, E. S., Richards, N. G., & Schuster, S. M. (1997). Mutagenesis and chemical
870 rescue indicate residues involved in beta-aspartyl-AMP formation by Escherichia coli
871 asparagine synthetase B. *The Journal of Biological Chemistry*, *272*(19), 12384–12392.
872 https://doi.org/10.1074/jbc.272.19.12384
873 Brachmann, C. B., Davies, A., Cost, G. J., Caputo, E., Li, J., Hieter, P., & Boeke, J. D. (1998). Designer
874 deletion strains derived from Saccharomyces cerevisiae S288C: A useful set of strains and
875 plasmids for PCR-mediated gene disruption and other applications. *Yeast*, *14*(2), 115–132.
876 https://doi.org/10.1002/(SICI)1097-0061(19980130)14:2<115::AID-YEA204>3.0.CO;2-2

877 Chen, A., Xie, Q., Lin, Y., Xu, H., Shang, W., Zhang, J., … Wang, Z. (2016). Septins are involved in nuclear
878 division, morphogenesis and pathogenicity in Fusarium graminearum. *Fungal Genetics and*
879 *Biology: FG & B*, *94*, 79–87. https://doi.org/10.1016/j.fgb.2016.07.005
880 Conn, P. M., Smithson, D. C., Hodder, P. S., Stewart, M. D., Behringer, R. R., Smith, E., … Janovick, J. A.
881 (2014). Transitioning pharmacoperones to therapeutic use: In vivo proof-of-principle and
882 design of high throughput screens. *Pharmacological Research*, *83*, 38–51.
883 https://doi.org/10.1016/j.phrs.2013.12.004
884 Dagdas, Y. F., Yoshino, K., Dagdas, G., Ryder, L. S., Bielska, E., Steinberg, G., & Talbot, N. J. (2012).
885 Septin-mediated plant cell invasion by the rice blast fungus, Magnaporthe oryzae. *Science (New*
886 *York, N.Y.)*, *336*(6088), 1590–1595. https://doi.org/10.1126/science.1222934
887 De Virgilio, C., DeMarini, D. J., & Pringle, J. R. (1996). SPR28, a sixth member of the septin gene family
888 in Saccharomyces cerevisiae that is expressed specifically in sporulating cells. *Microbiology*
889 *(Reading, England)*, *142 (Pt 10)*, 2897–2905.
890 Derkatch, I. L., Bradley, M. E., Zhou, P., Chernoff, Y. O., & Liebman, S. W. (1997). Genetic and
891 environmental factors affecting the de novo appearance of the [PSI+] prion in Saccharomyces
892 cerevisiae. *Genetics*, *147*(2), 507–519.
893 Dolat, L., Hu, Q., & Spiliotis, E. T. (2014). Septin functions in organ system physiology and pathology.
894 *Biological Chemistry*, *395*(2), 123–141. https://doi.org/10.1515/hsz-2013-0233
895 Dugdale, M. L., Vance, M. L., Wheatley, R. W., Driedger, M. R., Nibber, A., Tran, A., & Huber, R. E. (2010).
896 Importance of Arg-599 of β-galactosidase (Escherichia coli) as an anchor for the open
897 conformations of Phe-601 and the active-site loop. *Biochemistry and Cell Biology = Biochimie Et*
898 *Biologie Cellulaire*, *88*(6), 969–979. https://doi.org/10.1139/O10-144
899 Erives, A. J., & Fassler, J. S. (2015). Metabolic and chaperone gene loss marks the origin of animals:
900 Evidence for Hsp104 and Hsp78 chaperones sharing mitochondrial enzymes as clients. *PloS*
901 *One*, *10*(2), e0117192. https://doi.org/10.1371/journal.pone.0117192

902 Estey, M. P., Ciano-Oliveira, C. D., Froese, C. D., Bejide, M. T., & Trimble, W. S. (2010). Distinct roles of
903 septins in cytokinesis: SEPT9 mediates midbody abscission. *The Journal of Cell Biology*, *191*(4),
904 741–749. https://doi.org/10.1083/jcb.201006031
905 Fares, H., Goetsch, L., & Pringle, J. R. (1996). Identification of a developmentally regulated septin and
906 involvement of the septins in spore formation in Saccharomyces cerevisiae. *The Journal of Cell*
907 *Biology*, *132*(3), 399–411.
908 Farkasovsky, M., Herter, P., Voss, B., & Wittinghofer, A. (2005). Nucleotide binding and filament
909 assembly of recombinant yeast septin complexes. *Biological Chemistry*, *386*(7), 643–656.
910 https://doi.org/10.1515/BC.2005.075
911 Frank, J., Radermacher, M., Penczek, P., Zhu, J., Li, Y., Ladjadj, M., & Leith, A. (1996). SPIDER and WEB:
912 Processing and visualization of images in 3D electron microscopy and related fields. *Journal of*
913 *Structural Biology*, *116*(1), 190–199. https://doi.org/10.1006/jsbi.1996.0030
914 Fung, K. Y. Y., Dai, L., & Trimble, W. S. (2014). Cell and molecular biology of septins. *International*
915 *Review of Cell and Molecular Biology*, *310*, 289–339. https://doi.org/10.1016/B978-0-12-
916 800180-6.00007-4
917 Garcia, G., 3rd, Bertin, A., Li, Z., Song, Y., McMurray, M. A., Thorner, J., & Nogales, E. (2011). Subunit-
918 dependent modulation of septin assembly: Budding yeast septin Shs1 promotes ring and gauze
919 formation. *The Journal of Cell Biology*, *195*(6), 993–1004.
920 https://doi.org/10.1083/jcb.201107123
921 Garcia, G., Finnigan, G. C., Heasley, L. R., Sterling, S. M., Aggarwal, A., Pearson, C. G., … Thorner, J.
922 (2016). Assembly, molecular organization, and membrane-binding properties of development-
923 specific septins. *The Journal of Cell Biology*, *212*(5), 515–529.
924 https://doi.org/10.1083/jcb.201511029

925 Goedl, C., & Nidetzky, B. (2008). The phosphate site of trehalose phosphorylase from Schizophyllum
926 commune probed by site-directed mutagenesis and chemical rescue studies. *The FEBS Journal*,
927 *275*(5), 903–913. https://doi.org/10.1111/j.1742-4658.2007.06254.x
928 Guillén Schlippe, Y. V., & Hedstrom, L. (2005). Guanidine derivatives rescue the Arg418Ala mutation of
929 Tritrichomonas foetus IMP dehydrogenase. *Biochemistry*, *44*(50), 16695–16700.
930 https://doi.org/10.1021/bi051603w
931 Hartwell, L. H. (1971). Genetic control of the cell division cycle in yeast. IV. Genes controlling bud
932 emergence and cytokinesis. *Experimental Cell Research*, *69*(2), 265–276.
933 Heasley, L. R., & McMurray, M. A. (2016). Roles of septins in prospore membrane morphogenesis and
934 spore wall assembly in Saccharomyces cerevisiae. *Molecular Biology of the Cell*, *27*(3), 442–
935 450. https://doi.org/10.1091/mbc.E15-10-0721
936 Helfer, H., & Gladfelter, A. S. (2006). AgSwe1p Regulates Mitosis in Response to Morphogenesis and
937 Nutrients in Multinucleated Ashbya gossypii Cells. *Molecular Biology of the Cell*, *17*(10), 4494–
938 4512. https://doi.org/10.1091/mbc.E06-03-0215
939 Hernández-Rodríguez, Y., Hastings, S., & Momany, M. (2012). The septin AspB in Aspergillus nidulans
940 forms bars and filaments and plays roles in growth emergence and conidiation. *Eukaryotic Cell*,
941 *11*(3), 311–323. https://doi.org/10.1128/EC.05164-11
942 Hernández-Rodríguez, Y., Masuo, S., Johnson, D., Orlando, R., Smith, A., Couto-Rodriguez, M., &
943 Momany, M. (2014). Distinct Septin Heteropolymers Co-Exist during Multicellular
944 Development in the Filamentous Fungus Aspergillus nidulans. *PloS One*, *9*(3), e92819.
945 https://doi.org/10.1371/journal.pone.0092819
946 Ho, J., Tumkaya, T., Aryal, S., Choi, H., & Claridge-Chang, A. (2019). Moving beyond P values: Data
947 analysis with estimation graphics. *Nature Methods*, *16*(7), 565–566.
948 https://doi.org/10.1038/s41592-019-0470-3

949 Hung, J. E., Fogle, E. J., Garg, N., Chekan, J. R., Nair, S. K., & van der Donk, W. A. (2014). Chemical rescue
950 and inhibition studies to determine the role of Arg301 in phosphite dehydrogenase. *PloS One*,
951 *9*(1), e87134. https://doi.org/10.1371/journal.pone.0087134
952 Iwase, M., Luo, J., Bi, E., & Toh-e, A. (2007). Shs1 plays separable roles in septin organization and
953 cytokinesis in Saccharomyces cerevisiae. *Genetics*, *177*(1), 215–229.
954 https://doi.org/10.1534/genetics.107.073007
955 Johnson, C. R., Weems, A. D., Brewer, J. M., Thorner, J., & McMurray, M. A. (2015). Cytosolic chaperones
956 mediate quality control of higher-order septin assembly in budding yeast. *Molecular Biology of*
957 *the Cell*. https://doi.org/10.1091/mbc.E14-11-1531
958 Jones, G. W., Song, Y., & Masison, D. C. (2003). Deletion of the Hsp70 chaperone gene SSB causes
959 hypersensitivity to guanidine toxicity and curing of the [PSI+] prion by increasing guanidine
960 uptake in yeast. *Molecular Genetics and Genomics: MGG*, *269*(3), 304–311.
961 https://doi.org/10.1007/s00438-003-0838-y
962 Jung, G., & Masison, D. C. (2001). Guanidine hydrochloride inhibits Hsp104 activity in vivo: A possible
963 explanation for its effect in curing yeast prions. *Current Microbiology*, *43*(1), 7–10.
964 https://doi.org/10.1007/s002840010251
965 Kalia, J., & Swartz, K. J. (2011). Elucidating the molecular basis of action of a classic drug: Guanidine
966 compounds as inhibitors of voltage-gated potassium channels. *Molecular Pharmacology*, *80*(6),
967 1085–1095. https://doi.org/10.1124/mol.111.074989
968 Karasmanis, E. P., Phan, C.-T., Angelis, D., Kesisova, I. A., Hoogenraad, C. C., McKenney, R. J., & Spiliotis,
969 E. T. (2018). Polarity of Neuronal Membrane Traffic Requires Sorting of Kinesin Motor Cargo
970 during Entry into Dendrites by a Microtubule-Associated Septin. *Developmental Cell*, *46*(2),
971 204-218.e7. https://doi.org/10.1016/j.devcel.2018.06.013

Kermani, A. A., Macdonald, C. B., Gundepudi, R., & Stockbridge, R. B. (2018). Guanidinium export is the primal function of SMR family transporters. *Proceedings of the National Academy of Sciences of the United States of America*, *115*(12), 3060–3065. https://doi.org/10.1073/pnas.1719187115

Kim, M. S., Froese, C. D., Estey, M. P., & Trimble, W. S. (2011). SEPT9 occupies the terminal positions in septin octamers and mediates polymerization-dependent functions in abscission. *The Journal of Cell Biology*, *195*(5), 815–826. https://doi.org/10.1083/jcb.201106131

Kozubowski, L., & Heitman, J. (2010). Septins enforce morphogenetic events during sexual reproduction and contribute to virulence of Cryptococcus neoformans. *Molecular Microbiology*, *75*(3), 658–675. https://doi.org/10.1111/j.1365-2958.2009.06983.x

Kulak, N. A., Pichler, G., Paron, I., Nagaraj, N., & Mann, M. (2014). Minimal, encapsulated proteomic-sample processing applied to copy-number estimation in eukaryotic cells. *Nature Methods*, *11*(3), 319–324. https://doi.org/10.1038/nmeth.2834

Kuo, Y.-C., Shen, Y.-R., Chen, H.-I., Lin, Y.-H., Wang, Y.-Y., Chen, Y.-R., … Kuo, P.-L. (2015). SEPT12 orchestrates the formation of mammalian sperm annulus by organizing core octameric complexes with other SEPT proteins. *Journal of Cell Science*, *128*(5), 923–934. https://doi.org/10.1242/jcs.158998

Lehoux, I. E., & Mitra, B. (2000). Role of arginine 277 in (S)-mandelate dehydrogenase from Pseudomonas putida in substrate binding and transition state stabilization. *Biochemistry*, *39*(33), 10055–10065.

Leipe, D. D., Wolf, Y. I., Koonin, E. V., & Aravind, L. (2002). Classification and evolution of P-loop GTPases and related ATPases. *Journal of Molecular Biology*, *317*(1), 41–72. https://doi.org/10.1006/jmbi.2001.5378

Li, Z., Vizeacoumar, F. J., Bahr, S., Li, J., Warringer, J., Vizeacoumar, F. S., … Boone, C. (2011). Systematic exploration of essential yeast gene function with temperature-sensitive mutants. *Nature Biotechnology*, *29*(4), 361–367. https://doi.org/10.1038/nbt.1832

997 Lindquist, S. (2009). Protein folding sculpting evolutionary change. *Cold Spring Harbor Symposia on*
998 *Quantitative Biology*, *74*, 103–108. https://doi.org/10.1101/sqb.2009.74.043
999 Longtine, M. S., & Bi, E. (2003). Regulation of septin organization and function in yeast. *Trends in Cell*
1000 *Biology*, *13*(8), 403–409.
1001 Ludtke, S. J., Baldwin, P. R., & Chiu, W. (1999). EMAN: Semiautomated software for high-resolution
1002 single-particle reconstructions. *Journal of Structural Biology*, *128*(1), 82–97.
1003 https://doi.org/10.1006/jsbi.1999.4174
1004 McMurray, M. A. (2016). Assays for genetic dissection of septin filament assembly in yeast, from de
1005 novo folding through polymerization. *Methods in Cell Biology*, *136*, 99–116.
1006 https://doi.org/10.1016/bs.mcb.2016.03.012
1007 McMurray, M. A., Bertin, A., Garcia, G., 3rd, Lam, L., Nogales, E., & Thorner, J. (2011). Septin filament
1008 formation is essential in budding yeast. *Developmental Cell*, *20*(4), 540–549.
1009 https://doi.org/10.1016/j.devcel.2011.02.004
1010 McMurray, M. A., & Thorner, J. (2008). Septin stability and recycling during dynamic structural
1011 transitions in cell division and development. *Current Biology: CB*, *18*(16), 1203–1208.
1012 https://doi.org/10.1016/j.cub.2008.07.020
1013 Mendonça, D. C., Macedo, J. N., Guimarães, S. L., Barroso da Silva, F. L., Cassago, A., Garratt, R. C., …
1014 Araujo, A. P. U. (2019). A revised order of subunits in mammalian septin complexes.
1015 *Cytoskeleton (Hoboken, N.J.)*. https://doi.org/10.1002/cm.21569
1016 Michel, A. H., Hatakeyama, R., Kimmig, P., Arter, M., Peter, M., Matos, J., … Kornmann, B. (2017).
1017 Functional mapping of yeast genomes by saturated transposition. *ELife*, *6*.
1018 https://doi.org/10.7554/eLife.23570
1019 Mitchison, T. J., & Field, C. M. (2002). Cytoskeleton: What does GTP do for septins? *Current Biology: CB*,
1020 *12*(22), R788-790.

1021 Mostowy, S., & Cossart, P. (2012). Septins: The fourth component of the cytoskeleton. *Nature Reviews.*
1022 *Molecular Cell Biology*, *13*(3), 183–194. https://doi.org/10.1038/nrm3284
1023 Nagaraj, S., Rajendran, A., Jackson, C. E., & Longtine, M. S. (2008). Role of nucleotide binding in septin-
1024 septin interactions and septin localization in Saccharomyces cerevisiae. *Molecular and Cellular*
1025 *Biology*, *28*(16), 5120–5137. https://doi.org/10.1128/MCB.00786-08
1026 Nakahira, M., Macedo, J. N. A., Seraphim, T. V., Cavalcante, N., Souza, T. A. C. B., Damalio, J. C. P., …
1027 Kobarg, J. (2010). A draft of the human septin interactome. *PloS One*, *5*(11), e13799.
1028 https://doi.org/10.1371/journal.pone.0013799
1029 Nelson, J. W., Atilho, R. M., Sherlock, M. E., Stockbridge, R. B., & Breaker, R. R. (2017). Metabolism of
1030 Free Guanidine in Bacteria Is Regulated by a Widespread Riboswitch Class. *Molecular Cell*,
1031 *65*(2), 220–230. https://doi.org/10.1016/j.molcel.2016.11.019
1032 Nishihama, R., Onishi, M., & Pringle, J. R. (2011). New insights into the phylogenetic distribution and
1033 evolutionary origins of the septins. *Biological Chemistry*, *392*(8–9), 681–687.
1034 https://doi.org/10.1515/BC.2011.086
1035 Oh, S. J., Kim, D. S., Head, T. C., & Claussen, G. C. (1997). Low-dose guanidine and pyridostigmine:
1036 Relatively safe and effective long-term symptomatic therapy in Lambert-Eaton myasthenic
1037 syndrome. *Muscle & Nerve*, *20*(9), 1146–1152.
1038 Oh, Y., & Bi, E. (2011). Septin structure and function in yeast and beyond. *Trends in Cell Biology*, *21*(3),
1039 141–148. https://doi.org/10.1016/j.tcb.2010.11.006
1040 Onishi, M., & Pringle, J. R. (2016). The nonopisthokont septins: How many there are, how little we
1041 know about them, and how we might learn more. *Methods in Cell Biology*, *136*, 1–19.
1042 https://doi.org/10.1016/bs.mcb.2016.04.003
1043 Pablo-Hernando, M. E., Arnaiz-Pita, Y., Tachikawa, H., del Rey, F., Neiman, A. M., & Vázquez de Aldana,
1044 C. R. (2008). Septins localize to microtubules during nutritional limitation in Saccharomyces
1045 cerevisiae. *BMC Cell Biology*, *9*, 55. https://doi.org/10.1186/1471-2121-9-55

1046 Pan, F., Malmberg, R. L., & Momany, M. (2007). Analysis of septins across kingdoms reveals orthology
1047 and new motifs. *BMC Evolutionary Biology*, *7*, 103. https://doi.org/10.1186/1471-2148-7-103
1048 Pettersen, E. F., Goddard, T. D., Huang, C. C., Couch, G. S., Greenblatt, D. M., Meng, E. C., & Ferrin, T. E.
1049 (2004). UCSF Chimera—A visualization system for exploratory research and analysis. *Journal*
1050 *of Computational Chemistry*, *25*(13), 1605–1612. https://doi.org/10.1002/jcc.20084
1051 Phillips, M. A., Hedstrom, L., & Rutter, W. J. (1992). Guanidine derivatives restore activity to
1052 carboxypeptidase lacking arginine-127. *Protein Science: A Publication of the Protein Society*,
1053 *1*(4), 517–521. https://doi.org/10.1002/pro.5560010406
1054 Pinto, A. P. A., Pereira, H. M., Zeraik, A. E., Ciol, H., Ferreira, F. M., Brandão-Neto, J., … Araujo, A. P. U.
1055 (2017). Filaments and fingers: Novel structural aspects of the single septin from
1056 Chlamydomonas reinhardtii. *Journal of Biological Chemistry*, *292*(26), 10899–10911.
1057 https://doi.org/10.1074/jbc.M116.762229
1058 Pringle, J. R., Preston, R. A., Adams, A. E., Stearns, T., Drubin, D. G., Haarer, B. K., & Jones, E. W. (1989).
1059 Fluorescence microscopy methods for yeast. *Methods in Cell Biology*, *31*, 357–435.
1060 Qiao, Y., Molina, H., Pandey, A., Zhang, J., & Cole, P. A. (2006). Chemical rescue of a mutant enzyme in
1061 living cells. *Science (New York, N.Y.)*, *311*(5765), 1293–1297.
1062 https://doi.org/10.1126/science.1122224
1063 Rippert, D., & Heinisch, J. J. (2016). Investigation of the role of four mitotic septins and chitin synthase
1064 2 for cytokinesis in Kluyveromyces lactis. *Fungal Genetics and Biology: FG & B*, *94*, 69–78.
1065 https://doi.org/10.1016/j.fgb.2016.07.007
1066 Rynkiewicz, M. J., & Seaton, B. A. (1996). Chemical rescue by guanidine derivatives of an arginine-
1067 substituted site-directed mutant of Escherichia coli ornithine transcarbamylase. *Biochemistry*,
1068 *35*(50), 16174–16179. https://doi.org/10.1021/bi961311i
1069 Saarikangas, J., & Barral, Y. (2011). The emerging functions of septins in metazoans. *EMBO Reports*,
1070 *12*(11), 1118–1126. https://doi.org/10.1038/embor.2011.193

1071 *Saccharomyces Genome Database*. (n.d.). Retrieved from www.yeastgenome.org

1072 Sadeghipour, S., Bek, E. J., & McMinn, P. C. (2012). Selection and characterisation of guanidine-
1073 resistant mutants of human enterovirus 71. *Virus Research*, *169*(1), 72–79.
1074 https://doi.org/10.1016/j.virusres.2012.07.005

1075 Schaefer, R. M., Heasley, L. R., Odde, D. J., & McMurray, M. A. (2016). Kinetic partitioning during de
1076 novo septin filament assembly creates a critical G1 "window of opportunity" for mutant septin
1077 function. *Cell Cycle (Georgetown, Tex.)*, 0. https://doi.org/10.1080/15384101.2016.1196304

1078 Schneider, C. A., Rasband, W. S., & Eliceiri, K. W. (2012). NIH Image to ImageJ: 25 years of image
1079 analysis. *Nature Methods*, *9*(7), 671–675.

1080 Sellin, M. E., Holmfeldt, P., Stenmark, S., & Gullberg, M. (2011). Microtubules support a disk-like septin
1081 arrangement at the plasma membrane of mammalian cells. *Molecular Biology of the Cell*,
1082 *22*(23), 4588–4601. https://doi.org/10.1091/mbc.E11-09-0754

1083 Sellin, M. E., Sandblad, L., Stenmark, S., & Gullberg, M. (2011). Deciphering the rules governing
1084 assembly order of mammalian septin complexes. *Molecular Biology of the Cell*, *22*(17), 3152–
1085 3164. https://doi.org/10.1091/mbc.E11-03-0253

1086 Sellin, M. E., Stenmark, S., & Gullberg, M. (2014). Cell type-specific expression of SEPT3-homology
1087 subgroup members controls the subunit number of heteromeric septin complexes. *Molecular*
1088 *Biology of the Cell*, *25*(10), 1594–1607. https://doi.org/10.1091/mbc.E13-09-0553

1089 Shioya, T., Nakamura, H., Ishii, N., Takahashi, N., Sakamoto, Y., Ozaki, N., … Muraguchi, H. (2013). The
1090 Coprinopsis cinerea septin Cc.Cdc3 is involved in stipe cell elongation. *Fungal Genetics and*
1091 *Biology: FG & B*, *58–59*, 80–90. https://doi.org/10.1016/j.fgb.2013.08.007

1092 Sirajuddin, M., Farkasovsky, M., Hauer, F., Kühlmann, D., Macara, I. G., Weyand, M., … Wittinghofer, A.
1093 (2007). Structural insight into filament formation by mammalian septins. *Nature*, *449*(7160),
1094 311–315. https://doi.org/10.1038/nature06052

1095 Sirajuddin, M., Farkasovsky, M., Zent, E., & Wittinghofer, A. (2009). GTP-induced conformational
1096 changes in septins and implications for function. *Proceedings of the National Academy of*
1097 *Sciences of the United States of America*, *106*(39), 16592–16597.
1098 https://doi.org/10.1073/pnas.0902858106
1099 Soroor, F., Kim, M. S., Palander, O., Balachandran, Y., Collins, R., Benlekbir, S., … Trimble, W. S. (2019).
1100 Revised subunit order of mammalian septin complexes explains their in vitro polymerization
1101 properties. *BioRxiv*, 569871. https://doi.org/10.1101/569871
1102 Sweeny, E. A., & Shorter, J. (2016). Mechanistic and Structural Insights into the Prion-Disaggregase
1103 Activity of Hsp104. *Journal of Molecular Biology*, *428*(9 Pt B), 1870–1885.
1104 https://doi.org/10.1016/j.jmb.2015.11.016
1105 Trott, O., & Olson, A. J. (2010). AutoDock Vina: Improving the speed and accuracy of docking with a
1106 new scoring function, efficient optimization, and multithreading. *Journal of Computational*
1107 *Chemistry*, *31*(2), 455–461. https://doi.org/10.1002/jcc.21334
1108 Tuite, M. F., Mundy, C. R., & Cox, B. S. (1981). Agents that cause a high frequency of genetic change
1109 from [psi+] to [psi-] in Saccharomyces cerevisiae. *Genetics*, *98*(4), 691–711.
1110 Vargas-Muñiz, J. M., Renshaw, H., Richards, A. D., Lamoth, F., Soderblom, E. J., Moseley, M. A., …
1111 Steinbach, W. J. (2015). The Aspergillus fumigatus septins play pleiotropic roles in septation,
1112 conidiation, and cell wall stress, but are dispensable for virulence. *Fungal Genetics and Biology:*
1113 *FG & B*, *81*, 41–51. https://doi.org/10.1016/j.fgb.2015.05.014
1114 Versele, M., Gullbrand, B., Shulewitz, M. J., Cid, V. J., Bahmanyar, S., Chen, R. E., … Thorner, J. (2004).
1115 Protein-protein interactions governing septin heteropentamer assembly and septin filament
1116 organization in Saccharomyces cerevisiae. *Molecular Biology of the Cell*, *15*(10), 4568–4583.
1117 https://doi.org/10.1091/mbc.E04-04-0330
1118 Warenda, A. J., & Konopka, J. B. (2002). Septin function in Candida albicans morphogenesis. *Molecular*
1119 *Biology of the Cell*, *13*(8), 2732–2746. https://doi.org/10.1091/mbc.E02-01-0013

1120 Weems, A. D., Johnson, C. R., Argueso, J. L., & McMurray, M. A. (2014). Higher-Order Septin Assembly Is
1121 Driven by GTP-Promoted Conformational Changes: Evidence From Unbiased Mutational
1122 Analysis in Saccharomyces cerevisiae. *Genetics*, *196*(3), 711–727.
1123 https://doi.org/10.1534/genetics.114.161182
1124 Weems, A. D., & McMurray, M. A. (2017). The step-wise pathway of septin hetero-octamer assembly in
1125 budding yeast. *ELife*, *6*. https://doi.org/10.7554/eLife.23689
1126 Weirich, C. S., Erzberger, J. P., & Barral, Y. (2008). The septin family of GTPases: Architecture and
1127 dynamics. *Nature Reviews. Molecular Cell Biology*, *9*(6), 478–489.
1128 https://doi.org/10.1038/nrm2407
1129 Williams, D. M., Wang, D., & Cole, P. A. (2000). Chemical rescue of a mutant protein-tyrosine kinase.
1130 *The Journal of Biological Chemistry*, *275*(49), 38127–38130.
1131 https://doi.org/10.1074/jbc.C000606200
1132 Winzeler, E. A., Shoemaker, D. D., Astromoff, A., Liang, H., Anderson, K., Andre, B., … Davis, R. W.
1133 (1999). Functional Characterization of the S. cerevisiae Genome by Gene Deletion and Parallel
1134 Analysis. *Science*, *285*(5429), 901–906. https://doi.org/10.1126/science.285.5429.901
1135 Zent, E., & Wittinghofer, A. (2014). Human septin isoforms and the GDP-GTP cycle. *Biological*
1136 *Chemistry*, *395*(2), 169–180. https://doi.org/10.1515/hsz-2013-0268
1137 Zeymer, C., Werbeck, N. D., Schlichting, I., & Reinstein, J. (2013). The molecular mechanism of Hsp100
1138 chaperone inhibition by the prion curing agent guanidinium chloride. *The Journal of Biological*
1139 *Chemistry*, *288*(10), 7065–7076. https://doi.org/10.1074/jbc.M112.432583
1140 Zhang, Y. (2008). I-TASSER server for protein 3D structure prediction. *BMC Bioinformatics*, *9*, 40.
1141 https://doi.org/10.1186/1471-2105-9-40
1142
1143

1144 **Figure 1. GdnHCl rescues the temperature-sensitive defects of *cdc10(D182N)* mutants in a**
1145 **manner that does not require Hsp104 or Hsp78.**
1146 (A) Dilution series of yeast cells spotted on rich (YPD) agar medium with or without 3 mM GdnHCl
1147 and incubated at the indicated temperatures for 3 days before imaging. Strains were: BY4741,
1148 CBY07236, CBY06417, CBY08756, and CBY05110.
1149 (B) As in (A), but only at 37ºC and with strains of the indicated genotypes.
1150 (C) Amino acid alignment of regions *S. cerevisiae* Hsp104 and Hsp78 with *Thermus thermophilus*
1151 ClpB, showing conservation of residues (in red) that contact Gdm in the ClpB crystal structure (PDB
1152 4HSE).
1153 (D) As in (A), but at 37ºC and with BY4741 ("WT") or CBY06417 ("*cdc10(D182N)*") cells and the
1154 indicated concentrations of GdnHCl. The cells were streaked with a toothpick, rather than spotted
1155 from dilutions. (E) Growth curves for the *cdc10(D182N)* strain CBY06417 at 37ºC in the indicated
1156 concentrations of GdnHCl. The optical density at 600 nm ("OD_{600}") was measured at 5-min
1157 intervals. Each line shows the mean for 12 replicate cultures in the same row of the 96-well plate.
1158 Duplicate rows were monitored for each GdnHCl concentration.
1159
1160 **Figure 1–figure supplement 1. GdnHCl rescues high-temperature septin function and neck**
1161 **filament assembly in *cdc10* mutants.**
1162 (A) Dilution series of cells of the indicated genotypes (strains BY4741, CBY06417, CBY06420, or
1163 CBY06424) spotted on YPD plates with or without 3 mM GdnHCl and incubated at the indicated
1164 temperatures for 3-4 days.
1165 (B) anti-Cdc11 antibodies were used to stain *cdc10*Δ cells cultured at 37ºC in 3 mM GdnHCl.
1166 Arrowhead, septin ring.
1167 (C) Cells of the *cdc10(D182N)-GFP* strain JTY3986 were cultured at 37ºC in liquid YPD with 3 mM
1168 GdnHCl, cryo-fixed, cryo-substituted, sectioned, and stained with uranyl acetate prior to imaging by
1169 EM. Arrowheads indicate neck filaments tightly apposed to the plasma membrane.
1170 (D) As in (A), but with cells of strain BY4741 ("WT") or MMY0370 ("*cdc10*Δ *dpl1*Δ"). An intervening
1171 area of the plates was cropped from the images.
1172
1173 **Figure 2. GdnHCl promotes exclusion of mutant Cdc10 molecules from higher-order septin**
1174 **assemblies.**
1175 (A) As in Figure 1B, but with the addition of *cdc10*Δ cells, and the cells were streaked with a
1176 toothpick, rather than spotted from dilutions.
1177 (B) Cultures of the strains JTY3985 ("*CDC10-GFP*") or JTY3986 ("*cdc10(D182N)-GFP*") were grown

1178 overnight in liquid culture at the indicated temperatures with or without 3 mM GdnHCl and then
1179 imaged by microscopy with transmitted light (left images) or for GFP fluorescence (right images).
1180 Fluorescence images were inverted to improve visibility.
1181 (C) Cells of the strain JTY4020 were cultured at 37ºC with or without 5 mM GdnHCl and imaged as
1182 in (B), then linescans of bud neck fluorescence were performed for the indicated numbers of cells
1183 to quantify levels of Cdc10-mCherry (purple) or Cdc10(D182N)-GFP (green). For each data point,
1184 cytosolic signal was subtracted from bud neck signal; negative values thus indicate cytosolic signal
1185 greater than septin ring signal. In violin plots, solid lines indicate quartiles and dashed lines are
1186 medians.
1187 (D) In strain JTY5104, the chromosomal sources of Cdc3 and Cdc10 are eliminated by deletion and
1188 Cdc3(W364A) and Cdc10 are supplied by *LYS2*- or *URA3*-marked plasmids, respectively. Following
1189 introduction of *LEU2*-marked plasmid encoding WT Cdc3 (pFM831) or Cdc3-GFP (pML109), the
1190 transformants were passaged on medium with α-aminoadipate to select for loss of the
1191 *CDC3(W364A)* plasmid. These clones were then streaked, along with cells of the original strain
1192 JTY5104 carrying both plasmids ("*cdc10*Δ *CDC3(W364A)*"), on medium with 3 mM GdnHCl and 5-
1193 fluoro-orotic acid (FOA, to select for loss of the *CDC10* plasmid) and incubated for 4 days at 22ºC.
1194

1195 **Figure 3. GdnHCl promotes higher-order assembly by recombinant Cdc10-less septin**
1196 **hexamers produced in *E. coli*.**
1197 Complexes purified from *E. coli* cells co-expressing Cdc3, Cdc11, and 6xHis-Cdc12 in the absence
1198 or presence of 50 mM GdnHCl, as indicated, were examined with an electron microscope in (A)
1199 non-polymerizing ("high salt", 50 mM Tris-HCl pH 8, 300 mM NaCl with or without 50 mM GdnHCl)
1200 or (B) polymerizing ("low salt", 50 mM Tris-HCl pH 8, 50 mM NaCl with or without GdnHCl)
1201 conditions. Arrowheads point to complexes longer than trimers. Inserts in (A) display representative
1202 class averages resulting from image processing, with 10 nm scale bars. Insert in (B) shows the
1203 Fourier transform of a bundle of filaments as in the image beneath it, with arrows pointing at
1204 diffraction peaks reflecting repetitive distances of 27 nm.
1205 (C) As in (B) but with complexes synthesized and purified in the absence of GdnHCl to which
1206 GdnHCl was added to 50 mM prior to dilution in low salt buffer also containing 50 mM GdnHCl.
1207

1208 **Figure 4. Parallel *in silico* modeling and phylogenetic analysis independently point to Gdm**
1209 **binding near Thr302 and His262 in Cdc3.**
1210 (A) A model of the structure of Cdc3 based on SEPT2•GppNHp (PDB 3FTQ) was used for unbiased
1211 *in silico* docking of Gdm. The top 5 predicted sites of Gdm binding are shown (red), labeled with

1212 predicted free energies of binding, in kcal/mol. Thr302 is in blue, His262 in orange. "α4", α4 helix;
1213 "*t*L1", *trans* loop 1.
1214 (B) Cartoon ribbon view of human septin G homodimer crystal structures showing selected
1215 sidechains. Red, residues corresponding to the non-conservative changes seen in the phylogenetic
1216 analysis in Figure 4–figure supplement 1. Blue, conserved His residue of *trans* loop 1 and Asp
1217 residue of Switch II region. Orange, GTP analog. Red asterisk, Arg in α4 helix. "α4", α4 helix; "*t*L1",
1218 *trans* loop 1; "Sw1", Switch I; "Sw2", Switch II; "G1", G1 motif/P-loop.
1219
1220 **Figure 4–figure supplement 1. Co-variation during evolution of Cdc3 residues clustered**
1221 **around the *trans* loop 1 of the G dimerization interface identifies an Arg residue "missing"**
1222 **in species that poorly tolerate *cdc10*Δ.**
1223 Amino acid alignment of sequences of Cdc3 and its homologs in fungal species for which the
1224 phenotypic consequences of deletion or mutation of *CDC10* have been characterized in relation to
1225 deletion or mutation of *CDC3*. Names of species and the protein homologous to Cdc3 are color-
1226 coded: blue, species for which mutation of the *CDC10* homolog is as severe as mutation of the
1227 *CDC3* homolog; orange, species for which mutation of *CDC10* is clearly less severe than mutation
1228 of the *CDC3* homolog. Non-CTE human septin sequences are shown below for comparison with
1229 crystal structures of those septins shown in Figure 4B. Shading or boxing indicates residues that
1230 are either the same in *S. cerevisiae*, *A. gossypii*, and *K. lactis* and something different in the other
1231 fungal species, and/or the same in the other species and something different in *S. cerevisiae*, *A.*
1232 *gossypii*, and *K. lactis*. Gray, conservative changes; red, non-conservative changes. Red box:
1233 position 302 in ScCdc3. Key structural features are indicated above each group of sequences; "α0",
1234 α0 helix; "α4", a4 helix; "Sw I", Switch I loop; "G1", G1 motif; "G4", G4 motif. Sc, *S. cerevisiae*
1235 (KZV09558); Ag, *A. gossypii* (NP_985658); Kl, *K. lactis* (CAH00343), Ca, *C. albicans* (EEQ42751);
1236 An, *A. nidulans* (AAB41233); Cn, *C. neoformans* (XP_012050631); Fg, *F. graminearum*
1237 (ESU11253); Nc, *N. crassa* (ESA42882); Sp, *S. pombe* (CAB11714); Um, *U. maydis* (KIS68154);
1238 Mo, *M. oryzae* (ELQ45022); Cc, *C. cinerea* (XP_001828599); HsSEPT2, *H. sapiens* SEPT2
1239 (AAH33559); HsSEPT9, *H. sapiens* SEPT9 (AAH54004).
1240
1241 **Figure 5. GdnHCl rescues *cdc10*Δ in *A. gossypii.***
1242 *AgSHS1-GFP Agcdc10*Δ strain AG135 was grown with shaking for 15 hours at 37ºC in complete
1243 (AFM) medium, after which the culture was split in two and GdnHCl was added to one aliquot to
1244 30 mM final concentration. Cells were imaged after an additional 3 hours growth with shaking.
1245 Purple rectangles indicate the approximate region enlarged at right ("Zoom"). Scale bar, 10 μm.

1246

1247 **Figure 6. Partial rescue of TS defects by GdnHCl derivatives.**

1248 (A) WT strain BY4741 was cultured overnight in rich (YPD) medium containing the indicated
1249 concentrations of urea, and the density of each culture was determined with a spectrophotometer.
1250 (B) BY4741 ("WT") or the *cdc10(D182N)* strain CBY06417 ("*cdc10*") were streaked on plates
1251 containing no or 0.64 M urea and incubated at the indicated temperature for 3 days before imaging.
1252 (C) Cells from saturated YPD cultures of strains used in (A) were plated to form a monolayer on the
1253 surface of a rich (YPD) agar plate, and a 1-cm-diameter filter disk spotted with 5 µL of the indicated
1254 drug was placed in the center of the plate. The plate was imaged after incubation at 37ºC for 3 days.
1255 (D) As in Figure 1A, for strains of the indicated genotypes grown on medium containing 0 or 0.375
1256 mM of each indicated drug.
1257 (E) As in Figure 4A, but zoomed into the area between Thr302 and His262, and including the Gdm
1258 derivatives aminoguanidine ("aGdm") and N-ethylguanidine ("eGdm").
1259 (F) As in (B), but with the addition of strain CBY06420 ("*cdc10(G100E)*") and with arginine
1260 hydrochloride instead of urea.

1261

1262 **Figure 7. Arg at position 302 in Cdc3 blocks rescue of *cdc10* by GdnHCl.**

1263 As in Figure 2D, strain JTY5104 was transformed with a plasmid encoding GFP-tagged Cdc3
1264 (pML109) or derivatives in which the residue at position 302 was mutated from Thr to Val or Arg,
1265 followed by selection for loss of the plasmids encoding wild-type Cdc3 and Cdc10. Serial dilutions
1266 of the resulting strains were spotted on rich (YPD) medium at the indicated temperatures and
1267 containing GdnHCl where indicated, and imaged after 3 days.

1268

1269 **Figure 8. Reversing evolution to reactivate Cdc3 GTPase activity allows Cdc10 bypass**
1270 **during septin hetero-oligomerization.**

1271 (A) Strain MMY0130, which carries the mutations *cdc3(D210G) cdc10(D182N)*, was transformed
1272 with plasmid YCpK-Cdc10-1-GFP and cultured in rich (YPD) medium containing G-418 for plasmid
1273 selection in the presence or absence of GdnHCl. Bud neck fluorescence was measured as in Figure
1274 2B.
1275 (B) Haploid strains of the indicated genotypes expressing Cdc10-mCherry and Shs1-GFP were
1276 imaged as in (A) but in the absence of GdnHCl and for both mCherry and GFP fluorescence. For
1277 each cell, the ratio of mCherry to GFP signal was calculated; values are plotted on the left axis, with
1278 overlaid blue violin plots to show how the data are distributed, and median (dashed lines) and
1279 quartiles (solid lines) shown in green. The right axis shows the median difference ("effect size") for

1280 comparisons of the mutant strains against the shared wild-type control, plotted as bootstrap
1281 sampling distributions (gray violin plots). Each median difference is depicted as a block dot, with the
1282 value of that difference given in gray. Each 95% confidence interval is indicated by the ends of the
1283 vertical error bars. Strains were: MMY0342, MMY0343, and MMY0350.
1284 (C) Serial dilutions of the strains in (B) were spotted on rich (YPD) agar media with or without
1285 GdnHCl and incubated for 4 days at the indicated temperatures.
1286 (D) A portion of the *CDC10* coding sequence was amplified by PCR and sequenced. Asterisk in the
1287 chromatograph at left shows the mutation resulting in the amino acid change Q265H. Right,
1288 alignment of septin sequences surrounding the conserved Trp (bold) of the Sep4 motif and the His
1289 (bold) with which this Trp interacts across the G interface in the SEPT2 homodimer, as illustrated in
1290 (E). Red, Gln265 in wild-type Cdc10.
1291 (E) The Trp and His residues of the Sep4 motif in the SEPT2•GppNHp homodimer crystal structure
1292 (PDB 3FTQ).
1293
1294 **Figure 8–figure supplement 1. Sequence of the Cdc3-AspB chimeric protein and comparison**
1295 **of key residues between Cdc3, AspB, and Cdc12.**
1296 Alignments of *S. cerevisiae* Cdc3 with *Aspergillus nidulans* AspB and the Cdc3-AspB chimera
1297 (above), and with *S. cerevisiae* Cdc12 and *A. nidulans* AspB (below). Red highlighting indicates
1298 positions that covary with the catalytic Thr in Cdc3 homologs, as in Figure 4–figure supplement 1.
1299
1300 **Figure 8–figure supplement 2. Five substitutions in the GTPase domain of Cdc3 are**
1301 **insufficient to promote bypass of Cdc10 during septin assembly.**
1302 Strains of the indicated genotypes (JTY5397, MMY0361, MMY0362 and MMY0363) were grown to
1303 mid-logarithmic phase in liquid rich (YPD) medium and levels of Shs1-GFP and Cdc10-mCherry
1304 within septin rings were measured as in Figure 8B and plotted in (A) with effect size (median
1305 difference) distributions plotted in (B).
1306
1307 **Figure 9. Conservation of contacts between α4 Arg and *trans* loop 1 in the distant septin**
1308 **relative Toc34 and among *Candida* species, and drift at the α4 Arg position in**
1309 ***Saccharomyces* species.**
1310 (A) Structures of homodimer interface of Toc34 from *Arabidopsis thaliana*i (GppNHp-bound, PDB
1311 3bb3, top) and *Pisum sativum* (GDP-bound, PDB 1h65, bottom) with nucleotide in orange, α4 Arg
1312 in red and nucleotide-contacting *trans* loop 1 ("TL1") residues in blue.
1313 (B) Sequence alignment of a region in and around the α4 helix of Toc34 homologs in various plant

species, with identical and variable amino acids in black and red, respectively, and the α4 Arg in bold. *A. thaliania*, At (NP_196119); *A. lyrata*, Al (XP_002873181); *Camelina sativa*, Cs (XP_010423506); *Brassica napus*, Bn (CDX98810); *Noccaea caerulescens*, Nc (JAU73517); *B. rapa*, Br (XP_009130855); *Eutrema salsugineum*, Es (XP_006398957); *Vitis vinifera*, Vv (XP_002274573); *Eucalyptus grandis*, Eg (XP_010063039); *P. sativum*, Ps (Q41009); *Nicotiana tabacum*, Nt (XP_016456518); *Zea mays*, Zm (ACG34570).

(C) Sequence alignments of a region surrounding ScCdc3 Thr302 (highlighted in yellow), with identical and variable amino acids in black and red, respectively. Percent sequence identity over the entirety of Cdc3, relative to ScCdc3 or CaCdc3, is given at left. Alignments of *Saccharomyces* species were performed using the Saccharomyces Genome Database (http://www.yeastgenome.org). Sc, *S. cerevisiae*; Sp, *S. paradoxus*; Sm, *S. mikatae*; Sa, *S. aboricola*; Sb, *S. bayanus*; Su, *S. uvarum*; Sk, *S. kudriavzevii*. *Candida* alignments were performed at the NCBI Blast server. Ca, *C. albicans* (EEQ42751); Cd, *C. dubliniensis* (CAX44656); Cm, *C. maltosa* (EMG46918); Cr, *C. tropicalis* (XP_002550438); Ct, *C. tenuis* (EGV60285); Cg, *C. glabrata* (CAG57768).

Figure 9–figure supplement 1. Model for the roles of key molecular features during the evolution of septin complexes.

(A) A model of the evolution of septin hetero-octamers in *S. cerevisiae* from an ancestral homo-oligomer. Stars indicate the number of phosphate groups on bound nucleotide. Abbreviations: “CTE”, carboxy-terminal extension; “α4”, Arg and Asp residues of the α4 helix; “Sw2”, Switch II region; “*t*L1”, trans loop 1”.

(B) Illustration of the “revised” order of septin subunits in human hetero-octamers and hetero-hexamers, including the predicted phosphorylation state of bound nucleotides, as indicated by the number of black stars. SEPT9 is given as an example SEPT3-group subunit.

Table S1

Fungal strains used in this study.

Name* (species)	***Relevant genotype***	***Source/Reference***
(S.c.)[a]	*cdc10(D182N)-GFP::URA3 hsp78Δ::kanMX*	This study
(S.c.)[a]	*cdc10(D182N)-GFP::URA3 hsp104Δ::kanMX*	This study
(S.c.)[a]	*cdc10(D182N)-GFP::URA3 hsp78Δ::kanMX hsp104Δ::kanMX*	This study
Ag135 (A.g., also called AgHPH14)	*cdc10Δ::GEN1 SHS1-GFP–NAT1*	(Helfer & Gladfelter, 2006)
BY4741 (S.c.)	*MAT**a** his3Δ1 leu2Δ0 ura3Δ0 met15Δ0*	(Brachmann et al., 1998)
BY4742 (S.c.)	*MATα his3Δ1 leu2Δ0 ura3Δ0 lys2Δ0*	(Brachmann et al., 1998)
CBY05110 (S.c.)	BY4741 "*cdc12-1" cdc12(G247E)::KanMX*	(Li et al., 2011)
CBY06417 (S.c.)	BY4741 "*cdc10-1" cdc10(D182N)::KanMX*	(Li et al., 2011)
CBY06420 (S.c.)	BY4741 "*cdc10-2" cdc10(G100E)::KanMX*	(Li et al., 2011)
CBY06424 (S.c.)	BY4741 "*cdc10-5" cdc10(G44D)::KanMX*	(Li et al., 2011)
CBY06427 (S.c.)	BY4741 *cdc11(G29D)::KanMX*	(Li et al., 2011)
CBY07236 (S.c.)	BY4741 *"cdc3-3" cdc3(G365R)::KanMX*	(Li et al., 2011)
CBY08756 (S.c.)	BY4741 "*cdc11-1" cdc11(G32E I142T)::KanMX*	(Li et al., 2011)
JTY3985 (S.c.)	BY4741 *CDC10-GFP::URA3*	(Johnson et al., 2015)
JTY3986 (S.c.)	BY4741 *cdc10(D182N)-GFP::URA3*	(Johnson et al., 2015)
JTY3992 (S.c.)	BY4741 *CDC10-mCherry::KanMX*	(McMurray & Thorner, 2008)
JTY3993 (S.c.)	BY4742 *CDC10-mCherry::KanMX*	(McMurray & Thorner, 2008)
JTY4013 (S.c.)	BY4742 *hsp104Δ::kanMX*	(Winzeler et al., 1999)
JTY4014 (S.c.)	BY4741 *hsp104Δ::KanMX*	(Winzeler et al., 1999)
JTY4020[b] (S.c.)	BY4743 *CDC10-mCherry::kanMX/cdc10(D182N)-*	This study
JTY4203 (S.c.)	*cdc10Δ::kanMX* [*CDC10 URA3*]	(McMurray et al., 2011)
JTY5104 (S.c.)	*cdc3Δ cdc10Δ* [*CDC3(W364A) LYS2*] [*CDC10 URA3*]	(McMurray et al., 2011)
JTY5397 (S.c.)	BY4741 *CDC10-mCherry::kanMX SHS1-GFP::HIS3MX6*	(A. D. Weems & McMurray, 2017)
MMY0110 (S.c.)	*cdc3(D210G) cdc10(D182N)*	(A. D. Weems et al.,
MMY0130 (S.c.)	*cdc3(D210G) cdc10(D182N)*	(A. D. Weems et al.,
MMY0131 (S.c.)	*cdc3(D210G)*	(A. D. Weems et al.,
ATCC® 4013617 (S.c.)	BY4742 *hsp78Δ::kanMX*	(Winzeler et al., 1999)

MMY0343[c]	BY4741 *CDC10-mCherry::kanMX SHS1-GFP::HIS3MX6 cdc3(95-341)::aspB(6-234)*	This study
MMY0350[c]	BY4741 *cdc10(Q265H)-mCherry::kanMX SHS1-GFP::HIS3MX6 cdc3::aspB(6-234)*	This study
MMY0361[c]	BY4741 *CDC10-mCherry::kanMX SHS1-GFP::HIS3MX6 CDC3(P127E D128S K181T T302R Q306D)*	This study
MMY0362[c]	BY4741 *CDC10-mCherry::kanMX SHS1-GFP::HIS3MX6 CDC3"recoded"*	This study
MMY0363[c]	BY4741 *CDC10-mCherry::kanMX SHS1-GFP::HIS3MX6 CDC3(T302R Q306D)*	This study
Byk739	*ade2Δ::HIS3MX/ade2Δ::HIS3MX cdc10Δ::URA3/CDC10 dpl1Δ::natMX/DPL1 psd2Δ::kanMX/PSD2*	(Michel et al., 2017)
MMY0370	*ade2Δ::HIS3MX cdc10Δ::URA3 dpl1Δ::natMX PSD2*	This study

* Strains lacking names were generated by crossing other named strains or by selecting for loss of a plasmid from a named strain, and were used immediately thereafter. Their use in specific experiments in this study can be identified by their genotypes.

[a] Made by mating JTY3986 with the appropriate *hsp* deletion strain, or by mating of the *cdc10(D182N) hsp78Δ* strain with JTY4013, followed by sporulation and dissection of tetrads, then identification of genotypes via testing of marker phenotypes or segregation thereof (*e.g.* 2:2 segregation of G-418 resistance for *cdc10(D182N) hsp78Δ::kanMX hsp104Δ::kanMX*). Genotypes at other marker loci (*MAT*, *MET15*, *LYS2*, etc.) were not determined.

[b] Made by mating JTY3993 with JTY3985.

[c] Derived from JTY5397. See Methods section for details. Following confirmation of the integration via PCR and sequencing, spontaneous loss of plasmid pEM-CDC3-CRISPR1 was selected using 5-FOA.

[d] Made by sporulation of Byk739, dissection of asci, germination of spores, and analysis of markers to identify a spore clone of the appropriate genotype.

1355 **Table S2. Oligonucleotides used in this study.**

Name	Sequence (5' -> 3')
Cdc3AspBfw	GGTATGGGCATCACCTCCTCTCAGAGCGAAAAGG GTCAAGTTCTGCCTGACCAACCGGAGATTAAGTTC ATTCGCCGGAAGCTAACCGGC
Cdc3AspBextend1	GGAACGGCCTCTCACTTGATTACCGCTATAATTTT CCACGATGTCGTTGGAACCAATAACGGCAAAAGG AACCTTCGACAT
Cdc3GTPase_extend2	TTTCAAAAGGTTGAAATCAGAGTGGTTGTCATTGT CCACTTCGATCACCCCCCATGGATAGGAACGGCC TCTCACTTG
5'cdc3fw	AACTGAACGATTACATCGGC
3'cdc3re	TGTTTGAAATTTTTATATGTC
5'cdc10fw	CACGGTTACTACAAGCACTCT
3'cdc10re	TCACCACCATTCTTATGAGA
cdc10midfw	CCAAATGGAAAGGAGTTGAGC
CDC3GTPaserecode	ATTCGTCGTCAAATCAATGGTTATGTAGGGTTTGC TAATTTGCCCAAGCAATGGCACAGAAGGTCCATAA AGAACGGATTCAGTTTCAATCTCCTATGTGTCGGC GAGAGCGGTATAGGTAAGACAACATTAATGAAAAC ATTATTTAATAACGATGATATTGAAGCCAATTTAGT CAAAGATTACGAAGAGGAACTTGCTAATGATCAGG AGGAAGAGGAGGGACAGGGCGAGGGACACGAGA ACCAGTCACAAGAGCAAAGGCACACTGTCAAAAT CAAGTCATATGAGTCGGTTATTGAAGAAAATGGTG TTAAACTGAATTTGAACGTGATCGATACTGAAGGA TTTGGTGATTTTTTAAATAATGATCAAAAATCATGG GACCCGATCATTAAGGAGATTGACTCACGTTTTGA CCAATACTTAGATGCGGAGAATAAAATCAATAGAC ATTCTATAAACGACAAAAGAATCCACGCATGTCTA TATTTCATTGAGCCTACAGGACACTACTTAAAGCC GCTGGACCTTAAGTTTATGCAGTCAGTATATGAGA AATGTAATTTGATTCCTGTAATTGCTAAATCAGACA TCTTAACAGATGAAGAGATATTATCCTTCAAGAAG AGAATTATGAACGATTTAATACAATCAAATATAGAG CTTTTCAAACCACCAATATACTCCAACGATGACGC CGAAAATAGCCACTTGTCCGAAAGACTATTTTCCT CCTTACCTTACGCAGTTATTGGTTCAAATGACATC GTGGAAAATTATAGCGGTAATCAAGTGAGAGGCC GTTCCTATCCATGGGGGGTGATCGAAGTGGACAA TGACAACCACTCTGATTTCAACCTTTTGAAA
CDC3recode	ATTCGTCGTCAAATCAATGGTTATGTAGGGTTTGC TAATTTGCCCAAGCAATGGCACAGAAGGTCCATAA AGAACGGATTCAGTTTCAATCTCCTATGTGTCGGC CCTGATGGTATAGGTAAGACAACATTAATGAAAAC ATTATTTAATAACGATGATATTGAAGCCAATTTAGT CAAAGATTACGAAGAGGAACTTGCTAATGATCAGG AGGAAGAGGAGGGACAGGGCGAGGGACACGAGA

	ACCAGTCACAAGAGCAAAGGCACAAGGTCAAAAT CAAGTCATATGAGTCGGTTATTGAAGAAAATGGTG TTAAACTGAATTTGAACGTGATCGATACTGAAGGA TTTGGTGATTTTTTAAATAATGATCAAAAATCATGG GACCCGATCATTAAGGAGATTGACTCACGTTTTGA CCAATACTTAGATGCGGAGAATAAAATCAATAGAC ATTCTATAAACGACAAAAGAATCCACGCATGTCTA TATTTCATTGAGCCTACAGGACACTACTTAAAGCC GCTGGACCTTAAGTTTATGCAGTCAGTATATGAGA AATGTAATTTGATTCCTGTAATTGCTAAATCAGACA TCTTAACAGATGAAGAGATATTATCCTTCAAGAAG ACCATTATGAACCAGTTAATACAATCAAATATAGA GCTTTTCAAACCACCAATATACTCCAACGATGACG CCGAAAATAGCCACTTGTCCGAAAGACTATTTTCC TCCTTACCTTACGCAGTTATTGGTTCAAATGACAT CGTGGAAAATTATAGCGGTAATCAAGTGAGAGGC CGTTCCTATCCATGGGGGGTGATCGAAGTGGACA ATGACAACCACTCTGATTTCAACCTTTTGAAA
G1KTTRQDfw	ATTCGTCGTCAAATCAATGGTTATG
Cdc3recodere	TTTCAAAAGGTTGAAATCAGAGTGG

1356

Figure 1

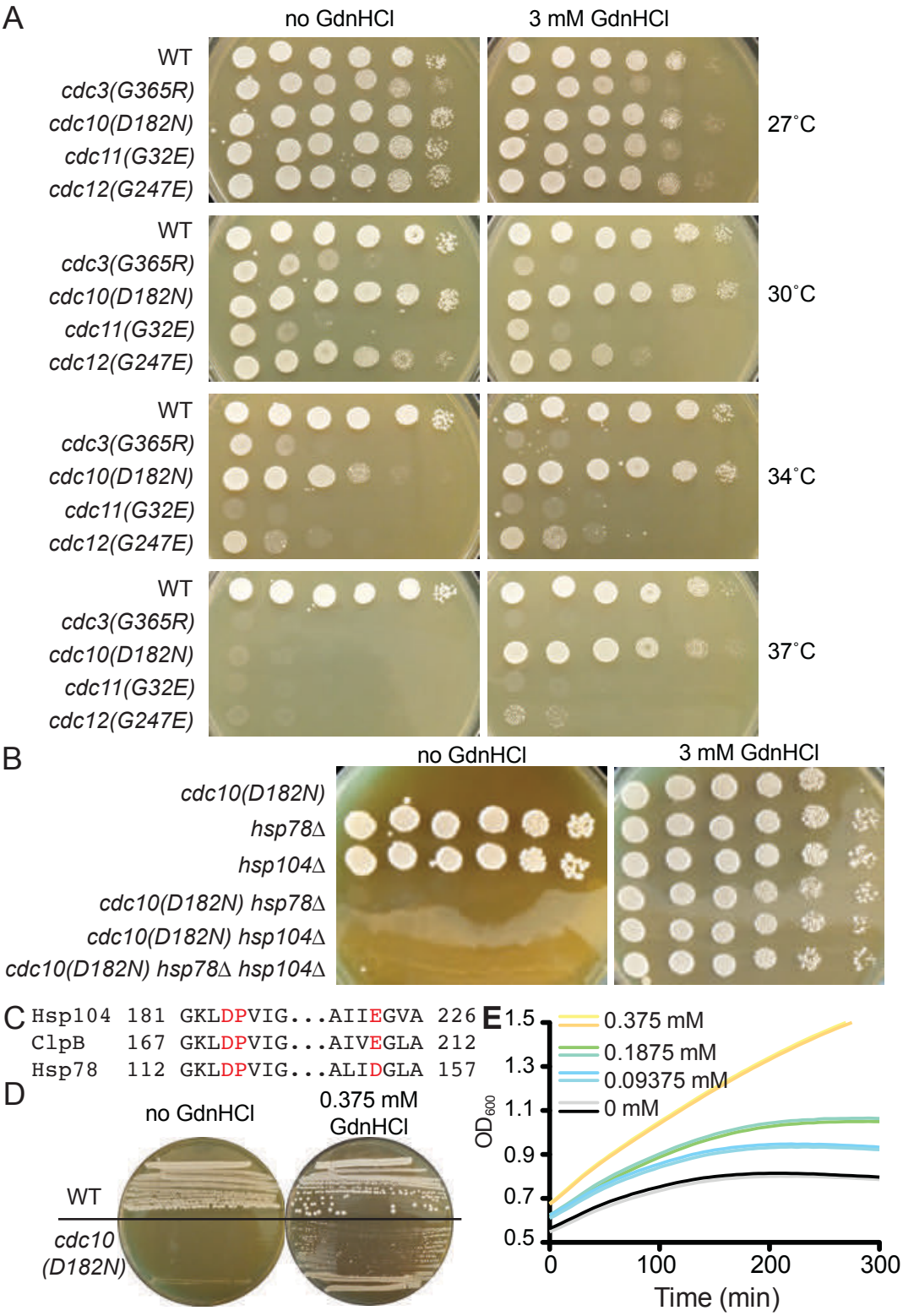
A
no GdnHCl
3 mM GdnHCl
WT
cdc3(G365R)
cdc10(D182N)
cdc11(G32E)
cdc12(G247E)
27˚C
30˚C
34˚C
37˚C
B
no GdnHCl
3 mM GdnHCl
cdc10(D182N)
hsp78Δ
hsp104Δ
cdc10(D182N) hsp78Δ
cdc10(D182N) hsp104Δ
cdc10(D182N) hsp78Δ hsp104Δ
C
Hsp104 181 GKLDPVIG...AIIEGVA 226
ClpB 167 GKLDPVIG...AIVEGLA 212
Hsp78 112 GKLDPVIG...ALIDGLA 157
D
no GdnHCl
0.375 mM GdnHCl
WT
cdc10 (D182N)
E
0.375 mM
0.1875 mM
0.09375 mM
0 mM
OD600
1.5
1.3
1.1
0.9
0.7
0.5
0
100
200
300
Time (min)

Figure 1-figure supplement 1

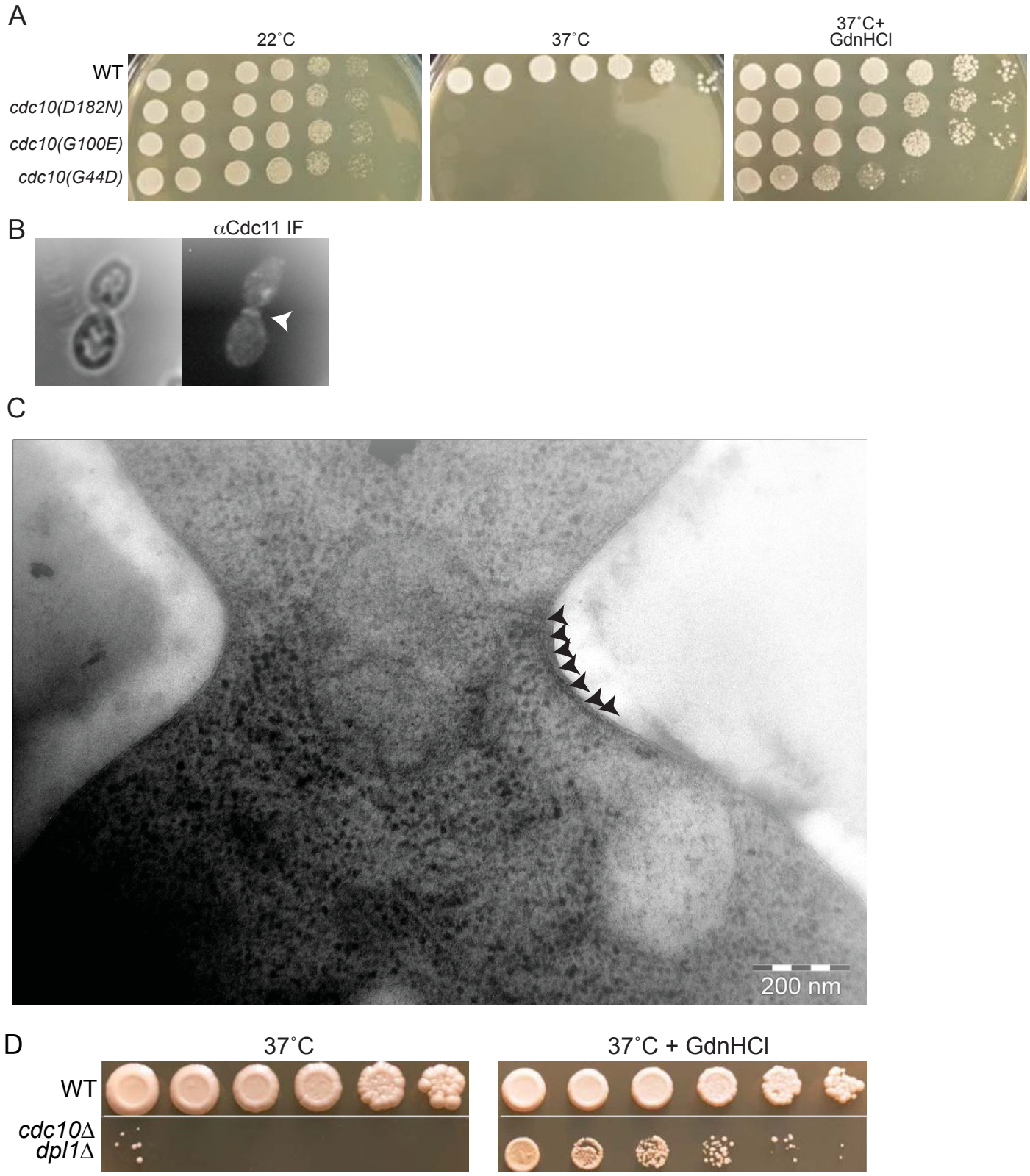

Figure 2

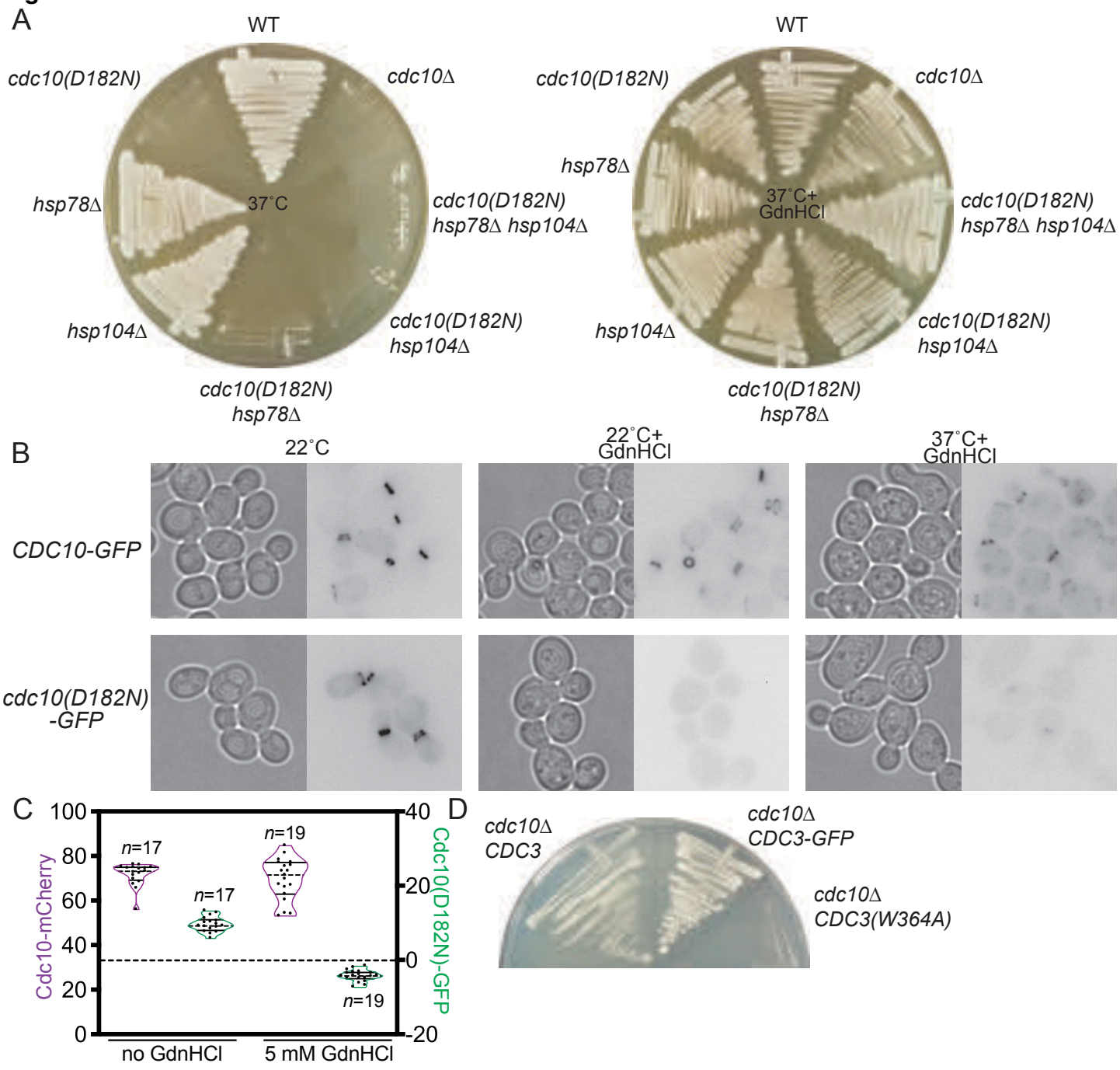
A
WT
cdc10(D182N)
cdc10Δ
hsp78Δ
37˚C
cdc10(D182N)
hsp78Δ hsp104Δ
hsp104Δ
cdc10(D182N)
hsp104Δ
cdc10(D182N)
hsp78Δ
WT
cdc10(D182N)
cdc10Δ
hsp78Δ
37˚C+
GdnHCl
cdc10(D182N)
hsp78Δ hsp104Δ
hsp104Δ
cdc10(D182N)
hsp104Δ
cdc10(D182N)
hsp78Δ
B
22˚C
22˚C+
GdnHCl
37˚C+
GdnHCl
CDC10-GFP
cdc10(D182N)
-GFP
C
Cdc10-mCherry
Cdc10(D182N)-GFP
n=17
n=17
n=19
n=19
100
80
60
40
20
0
40
20
0
-20
no GdnHCl
5 mM GdnHCl
D
cdc10Δ
CDC3
cdc10Δ
CDC3-GFP
cdc10Δ
CDC3(W364A)

Figure 3

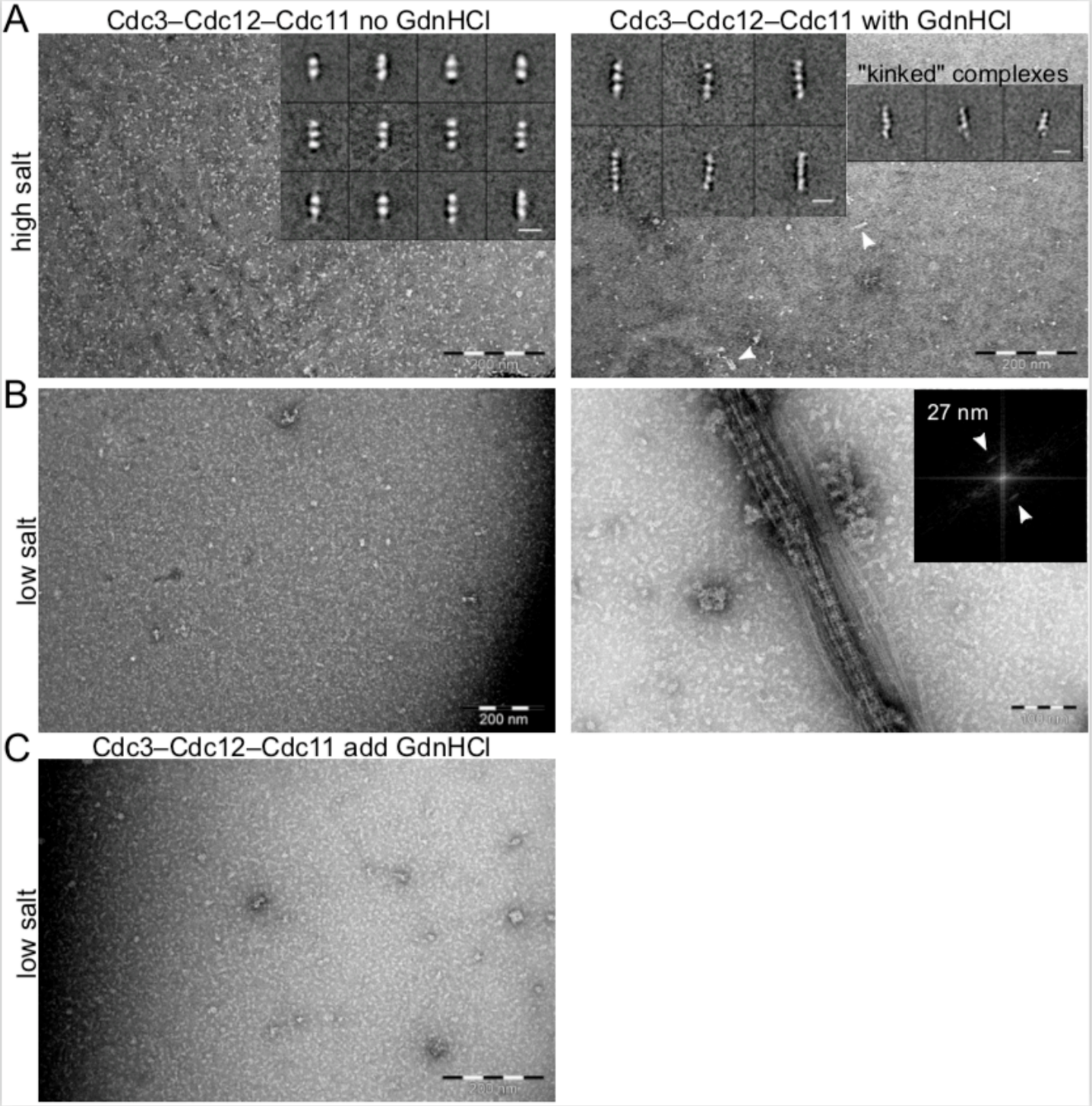
A
Cdc3–Cdc12–Cdc11 no GdnHCl
Cdc3–Cdc12–Cdc11 with GdnHCl
high salt
"kinked" complexes
200 nm
B
low salt
27 nm
200 nm
C
Cdc3–Cdc12–Cdc11 add GdnHCl
low salt
200 nm

Figure 4

A

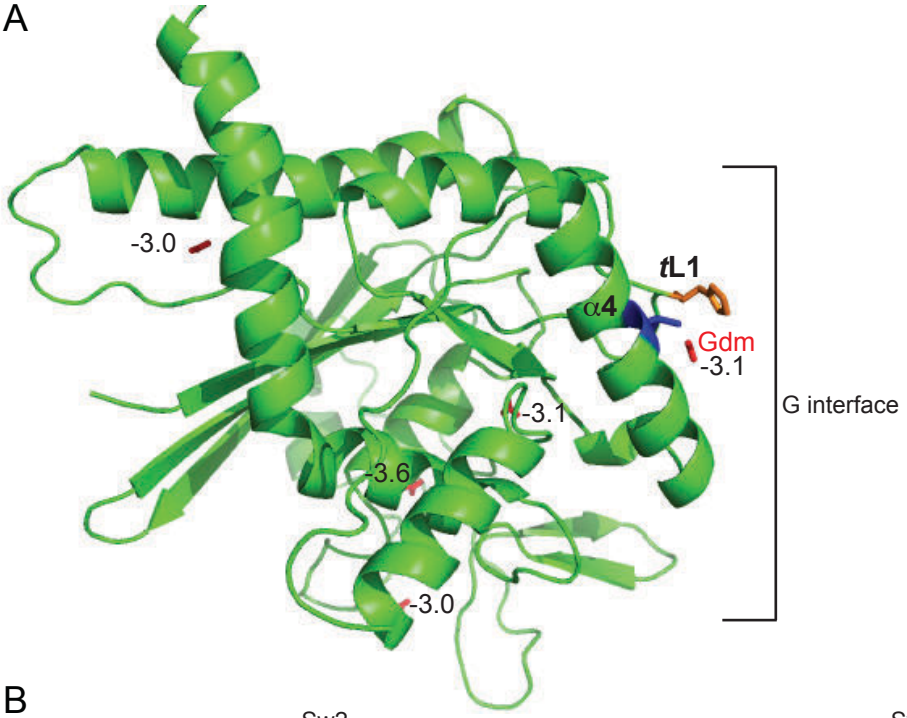

B

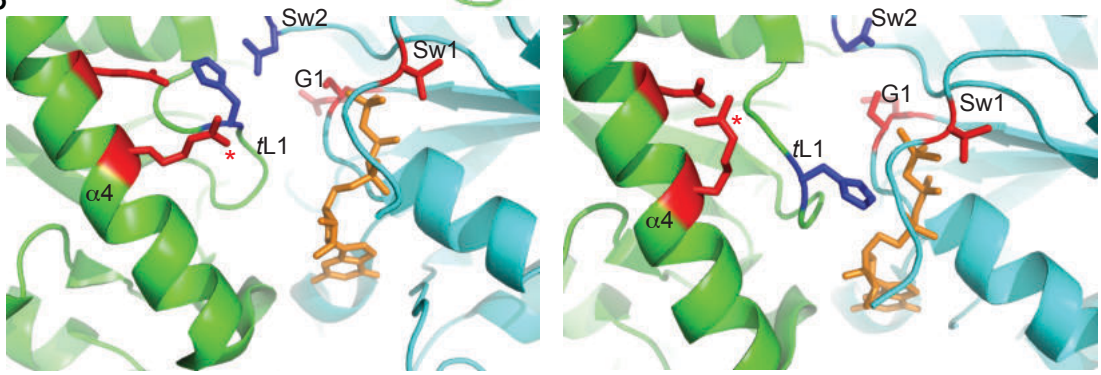

SEPT2•GppNHp SEPT9•GTPγS

Figure 4–figure supplement 1

```
                    (    α0     )            ---G1---
ScCdc3    95 QINGYVGFANLPKQWHRRSIKNGFSFNLLCVGPDGIGKTTLMKTLFNN  142
AgCdc3    89 KISGYVGFANLPKQWHRKSIRRGFNLNLLCVGAKGLGKSTLINTLFNK  136
KlCdc3    74 IINGYVGFANLPKQWHRKSIRRGFNLNLLCVGYKGLGKSTLINTLFNR  121
CaCdc3    23 VLNGYVGFANLPKQWHRKSIRRGFSLNIMAIGESGLGKATLINTLFNR  70
CcAspB    40 KLMGYVGFANLPNQVHRKSVRKGFQFTCMVVGESGLGKSTLVNTLFNT  87
UmCdc3    29 KLMGYVGFANLPNQVHRKSVRKGFNFTAMVVGESGLGKSTLINTLFNT  76
NcCdc3    60 KLTGYVGFANLPNQWHRKSVRKGFNFNVMVVGESGLGKSTLVNTLFNT  107
AnAspB     8 KLTGYVGFANLPNQWHRKSVRKGFNFNVMVVGESGLGKSTLVNTLFNT  55
MoSep3    46 KLTGYVGFANLPNQWHRKSVRKGFNFNVMVVGESGLGKSTLVNTLFNT  93
FgCdc3   165 KLTGYVGFANLPNQWHRKSVRKGFNFNVMVVGESGLGKSTLVNTLFNT  212
CnCdc3    60 KLSSWVGFSNLPNQVHRRSVRRGFQFVTMVVGESGLGKSTLINTLFET  107
SpSpn1    71 QLNGYVGFASLPNQWHRRCVRQGFNFNVLVLGESGSGKSTLVNTLLNR  118
HsSEPT2   12 ETPGYVGFANLPNQVHRKSVKKGFEFTLMVVGESGLGKSTLINSLFLT  60
HsSEPT9  256 VDFGYVGIDSILEQMRRKAMKQGFEFNIMVVGQSGLGKSTLINTLFKS  303

             -Sw I--                          -G4-   (      α4       )
ScCdc3   179 RHKVKIKSYESVIEE ... 278 KCNLIPVIAKSDILTDEEILSFKKTIMNQLIQSNIEL
AgCdc3   169 ENKVKIETVTTEIEE ... 267 KCNLIPVIAKSDILTDEEIEHFKWTIKKQLDDAKVHL
KlCdc3   160 ENKVKIETVSAEIEE ... 258 KCNLIPVIAKSDILTDEEIVTFKATIKKQLEQANVQL
CaCdc3    89 DVSVKIKSTQAEIEE ... 187 KVNLIPVIAKSDTLTDEEILEFKHRILADISHQGIKI
CcAspB   103 PKTVAIESIGADIEE ... 201 KVNLIPVIAKADTLTDEEVAEFKQRILADIAHHNIHI
UmCdc3    92 PKTVAIESISSDIEE ... 190 KVNLIPVIAKSDTLTDEEIVSFKQRILNDIAHHKIEI
NcCdc3   124 PKTVTIQSISADIEE ... 222 KVNLIPVIAKSDTLTDDEIAAFKARILADIKYHKVQI
AnAspB    72 PKTVSIQSISADIEE ... 170 KVNLIPVIAKADTLTDDEISMFKKRILADIQHHSIQI
MoSep3   110 PKTVTIQSISADIEE ... 208 KVNLIPVIAKSDTLTDEEIFAFKQRILADIKHHKVQI
FgCdc3   229 PKTVTIQSISADIEE ... 327 KVNLIPVIAKADTLTDEEIAAFKSRILADIKHHGIQI
CnCdc3   123 GKTVQIESISADIEE ... 221 KVNLIPIIAKADTMTDDEIIAFKQRILADIAHYGIQI
SpSpn1   137 EPTVMINSSAVEIVE ... 235 KVNIIPIIAKADTLTDDELNFTKEMILRDIQYHNIRI
HsSEPT2   76 ERTVQIEASTVEIEE ... 174 KVNIVPVIAKADTLTLKERERLKKRILDEIEEHNIKI
HsSEPT9  319 PKTIEIKSITHDIEE ... 272 VVNIVPVIAKADTLTLEERVHFKQRITADLLSNGIDV

              | C-terminal extension ->
ScCdc3   437  HEAKLAKLEIEMKTVF ... KEKLTKQLKALEDKK  516
AgCdc3   426  HEAKLAKLEAEMKAVF ... KEKLMKQLKALEEKK  502
KlCdc3   415  HEVKLAKLEAEMKAVF ... KDKLTSQLKALEEKK  491
CaCdc3   345  HEAKLAKMEAEMKSVF ... KDKLTKQIKLLEEKK  424
CcAspB   360  HEAKLAKMEAEMKMVF ... KDALEKQRAELEDKK  436
UmCdc3   349  HEARLRKMENEMKLVF ... RDALEKQRQELEEKR  425
NcCdc3   381  HEQKLAKMEAEMKMVF ... KEQLERQRLELEEKK  453
AnAspB   329  HEQKLAKMEAEMKMVF ... KEQLDRQRAELEEKK  400
MoSep3   367  HEQKLAKMEAEMKLVF ... KEQLDRQRAELEEKK  438
FgCdc3   486  HEQKLAKMEAEMKMVF ... KEQLDRQRLELEDKK  557
CnCdc3   380  HEAKLAKMEAEMKIVF ... KDALEKQKQELEDKR  456
SpSpn1   393  HEEKLMKMEAEMKTIF ... KAALEKQKADLIDHK  464
```

Figure 5

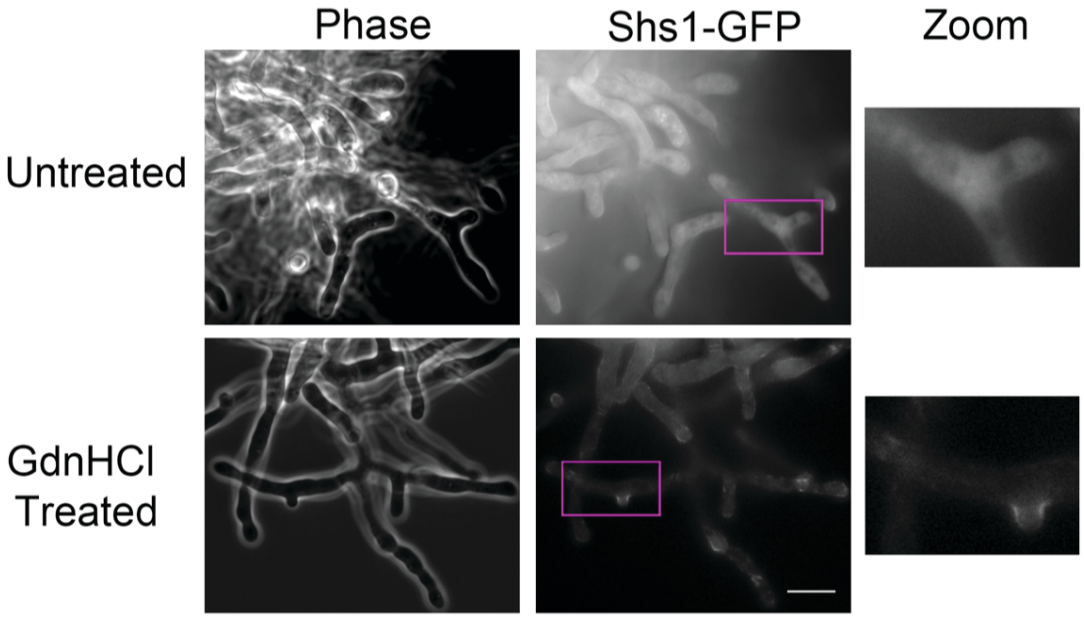

Figure 6

A

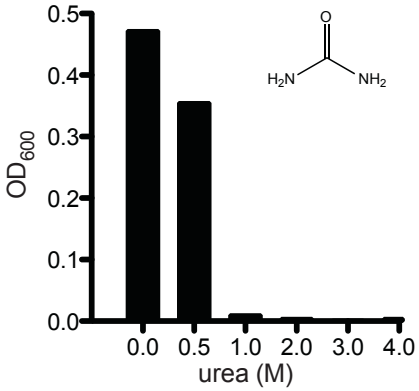

B

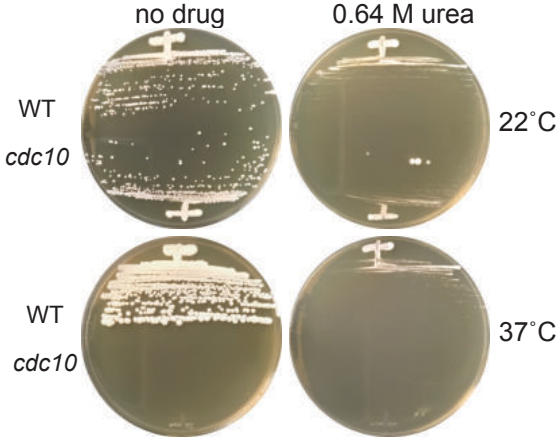

C

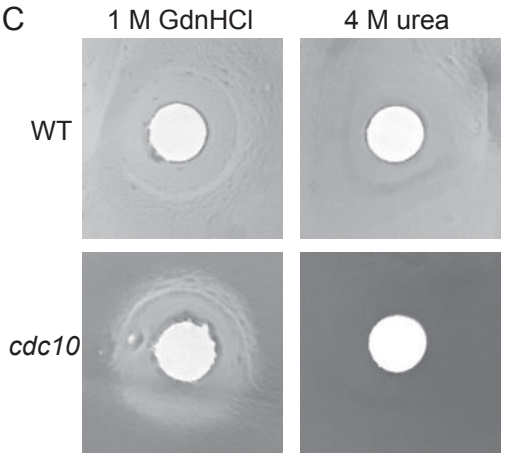

D

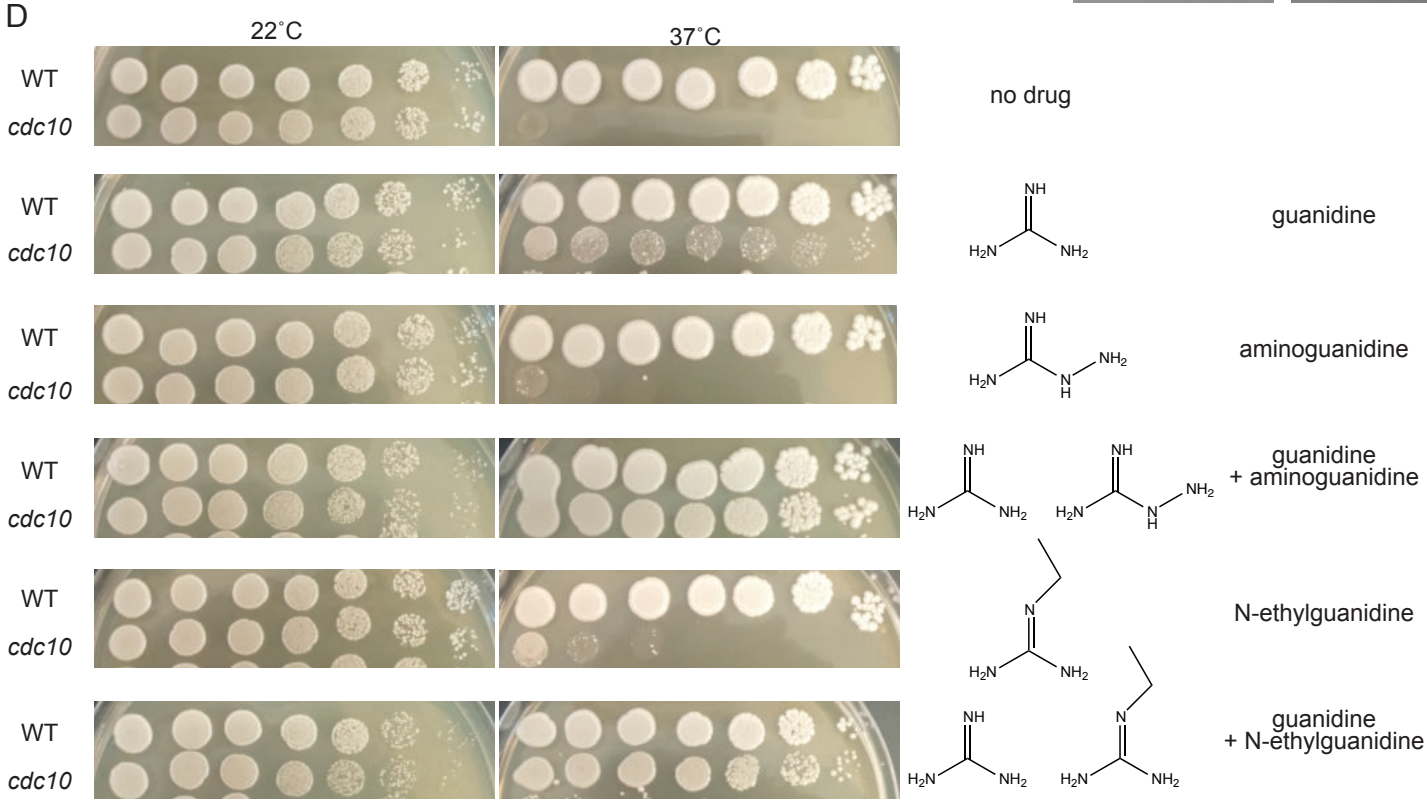

E

F

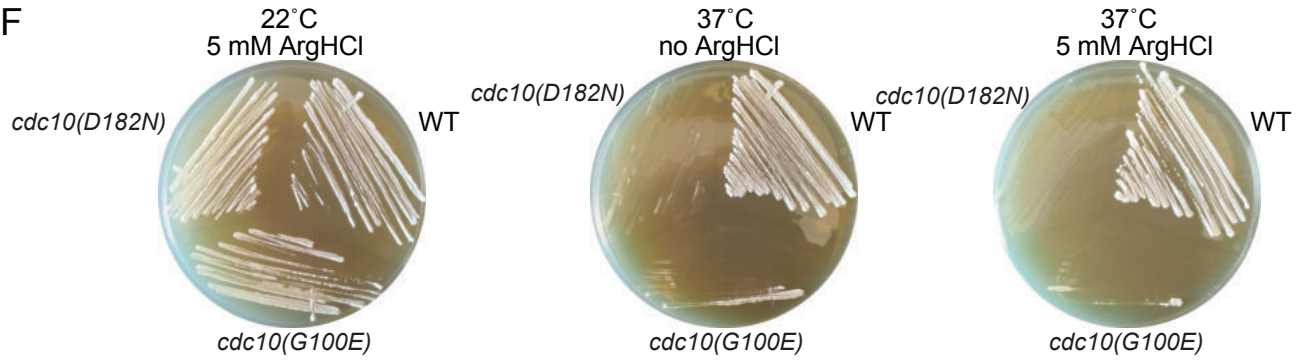

Figure 7

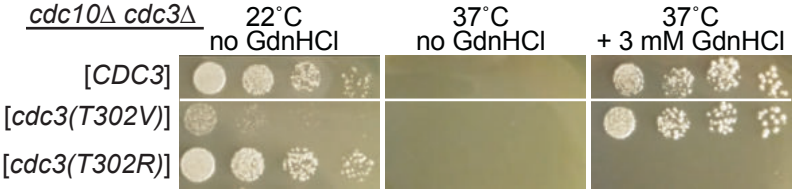
cdc10Δ cdc3Δ
22˚C
no GdnHCl
37˚C
no GdnHCl
37˚C
+ 3 mM GdnHCl
[CDC3]
[cdc3(T302V)]
[cdc3(T302R)]

Figure 8

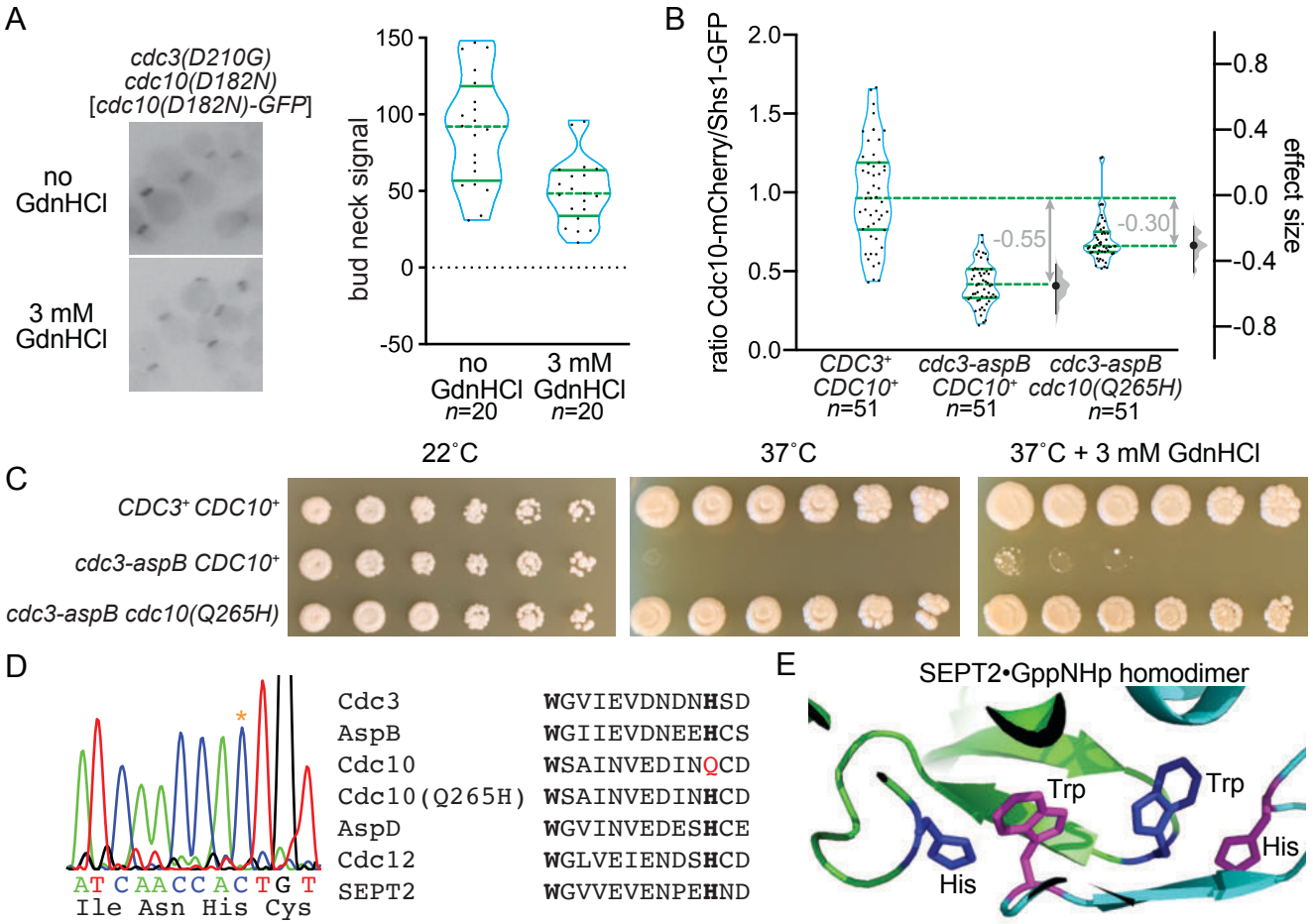
A
cdc3(D210G)
cdc10(D182N)
[cdc10(D182N)-GFP]
no GdnHCl
3 mM GdnHCl
bud neck signal
150
100
50
0
-50
no GdnHCl n=20
3 mM GdnHCl n=20
B
ratio Cdc10-mCherry/Shs1-GFP
2.0
1.5
1.0
0.5
0.0
effect size
0.8
0.4
0.0
-0.4
-0.8
-0.55
-0.30
CDC3+ CDC10+ n=51
cdc3-aspB CDC10+ n=51
cdc3-aspB cdc10(Q265H) n=51
C
22˚C
37˚C
37˚C + 3 mM GdnHCl
CDC3+ CDC10+
cdc3-aspB CDC10+
cdc3-aspB cdc10(Q265H)
D
AT C AACC AC T G T
Ile Asn His Cys
Cdc3 WGVIEVDNDNHSD
AspB WGIIEVDNEEHCS
Cdc10 WSAINVEDINQCD
Cdc10(Q265H) WSAINVEDINHCD
AspD WGVINVEDESHCE
Cdc12 WGLVEIENDSHCD
SEPT2 WGVVEVENPEHND
E
SEPT2•GppNHp homodimer
Trp
Trp
His
His

Figure 8–figure supplement 1

```
Cdc3-AspB  1    MSLKEEQVSIKQDPEQEERQHDQFNDVQIKQESQDHDGVDSQYTNGTQNDDSERFEAAESDVKVEPGLGMGITSSQSEKG  80
AspB            ------------------------------------------------------------------------------
Cdc3       1    MSLKEEQVSIKQDPEQEERQHDQFNDVQIKQESQDHDGVDSQYTNGTQNDDSERFEAAESDVKVEPGLGMGITSSQSEKG  80

Cdc3-AspB  81   QVLPDQPEIKFIRRKLTGYVGFANLPNQWHRKSVRKGFNFNVMVVGESGLGKSTLVNTLFNTSL    YPPKERAGPSHD  156
AspB       1    -------MKNVVRRKLTGYVGFANLPNQWHRKSVRKGFNFNVMVVGESGLGKSTLVNTLFNTSL    YPPKERAGPSHD  69
Cdc3       81   QVLPDQPEIKFIRRQINGYVGFANLPKQWHRRSIKNGFSFNLLCVGPDGIGKTTLMKTLFNNDD[16]QEEEEGQGEGHE  172

Cdc3-AspB  157  IIPK   TVSIQSISADIEENGVRLRLTVVDTPGFGDFVNNDD-SWRPIVENIEQRYDAYLEAENKVNRTNIIDNRIHAC  232
AspB       70   IIPK   TVSIQSISADIEENGVRLRLTVVDTPGFGDFVNNDD-SWRPIVENIEQRYDAYLEAENKVNRTNIIDNRIHAC  145
Cdc3       173  NQSQ[4]KVKIKSYESVIEENGVKLNLNVIDTEGFGDFLNNDQKSWDPIIKEIDSRFDQYLDAENKINRHSINDKRIHAC  253

Cdc3-AspB  233  VYFIQPTGHSLKPLDIEVMRRLHTKVNLIPVIAKADTLTDDEISMFKKRILADIQHHSIQIFEGPRYELDDEETIAENQE  312
AspB       146  VYFIQPTGHSLKPLDIEVMRRLHTKVNLIPVIAKADTLTDDEISMFKKRILADIQHHSIQIFEGPRYELDDEETIAENQE  225
Cdc3       254  LYFIEPTGHYLKPLDLKFMQSVYEKCNLIPVIAKSDILTDEEILSFKKTIMNQLIQSNIELFKPPIYSNDDAENSHLSER  333

Cdc3-AspB  313  IMSKVPFAVIGSNDIVENYSGNQVRGRSYPWGVIEVDNDNHSDFNLLKNLLIKQFMEELKERTSKILYENYRSSKLAKLG  392
AspB       226  IMSKVPFAVVGANSEVATSDGRKVRGRSYPWGIIEVDNEEHCSFVKLRQMLIRTHMEELKEHTNNHLYENYRSDKLTQMG  305
Cdc3       334  LFSSLPYAVIGSNDIVENYSGNQVRGRSYPWGVIEVDNDNHSDFNLLKNLLIKQFMEELKERTSKILYENYRSSKLAKLG  413

Cdc3-AspB  393  IKQDNSVFKEFDPISKQLEEKTLHEAKLAKLEIEMKTVFQQKVSEKEKKLQKSETELFARHKEMKEKLTKQLKALEDKKK  472
AspB       306  VAQDPSVFKEVNPAVKQEEEDALHEQKLAKMEAEMKMVFQQKVAEKESKLKQSEDELYARHREMKEQLDRQRAELEEKKA  385
Cdc3       414  IKQDNSVFKEFDPISKQQEEKTLHEAKLAKLEIEMKTVFQQKVSEKEKKLQKSETELFARHKEMKEKLTKQLKALEDKKK  493

Cdc3-AspB  473  QLELSINSASPNVNHSPVPTKKKGF-LR*  500
AspB       386  RLE----SGRPLEEKG----KRKGFSLR*  405
Cdc3       494  QLELSINSASPNVNHSPVPTKKKGF-LR*  521
```

```
         ---G1---       -Sw I--      α4        )
ScCdc3   GPDGIGKTT ... RHKVKIK ... KKTIMNQLIQ
ScCdc12  GESGLGKTT ... RKTVEID ... KSRIRQVIEA
AnAspB   GESGLGKST ... PKTVSIQ ... KQRILADIKH
```

Figure 8–figure supplement 2

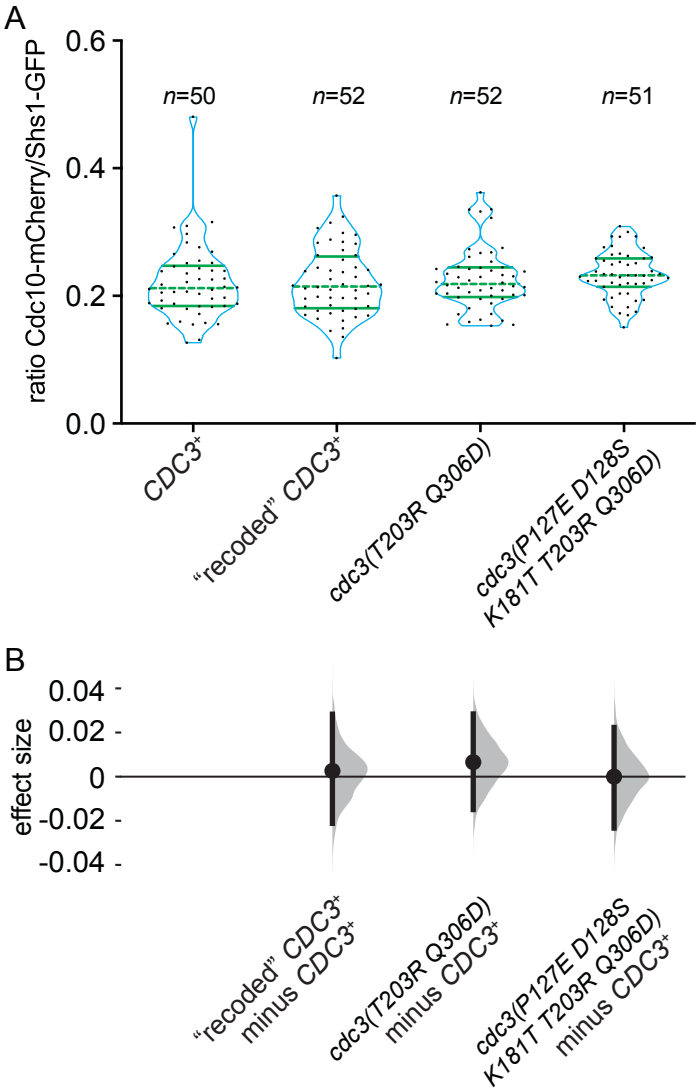

Figure 9

A

A. thaliana Toc34

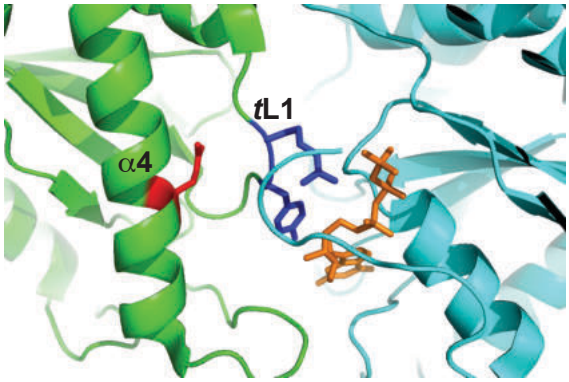

P. sativum Toc34

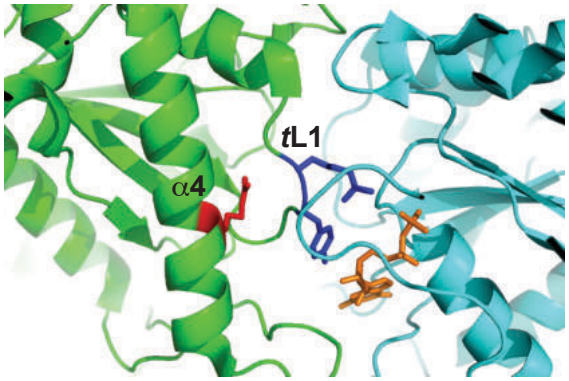

B

```
                          (          α4
At 160   LTHAQFSPPDGLNYNHFVSKRSNALL
Al 160   LTHAQFSPPDGLNYNSFVSRRSDALL
Cs 160   LTHAQFSPPDGLNYDLFVSRRSDALL
Bn 160   LSHAQFSPPDGLNYDLFVSRRSDALL
Nc 160   LTHAQFSPPDGLNYDLFVSRRSDALL
Br 160   LSHAQFSPPDGLNYDLFVSRRSDALL
Es 160   LSHAQFSPPDGLNYDLFVSRRSDALL
Vv 159   LTHAQLSPPDGLNYEDFFSKRSEALM
Eg 159   LTHAQLSPPDGLEYDLFFSKRSEALM
Ps 161   LTHAQFSPPDGLPYDEFFSKRSEALL
Nt 159   LSHAQLSPPDGLTYDEFTSQRSEALL
Zm 159   LTHAQLSPPDGIDYNDFFTRRSEALL
```

C

Cdc3 in *Saccharomyces* versus *Candida*

```
Sc       AKSDILTDEEILSFKKTIMNQLIQSNIELFKP  317
Sp 95%   AKSDILTDEEILSFKKTIMNQLIQSNIELFKP  313
Sm 89%   AKSDILTDEEILNFKKAIMNQLIQSNIELFKP  313
Sa 87%   AKSDILTDEEILNFKKTIMNQLVQSDIKLFKP  312
Sb 86%   AKSDILTDEEILNFKKSIMGQLAQSNIELFKP  375
Su 86%   AKSDILTDEEILNFKKSIMGQLAQSNIELFKP  375
Sk 86%   AKSDILTDEEILNFKKAIMNQLIESNIKLFKP  313

Ca       AKSDTLTDEEILEFKHRILADISHQGIKIFKP  226
Cd 99%   AKSDTLTDEEILEFKHRILADISHQGIKIFKP  226
Cm 91%   AKSDTLTDEEILEFKHRILADITHQGIKIFQP  225
Cr 90%   AKSDTLTDEEILEFKHRILADITYQGIKIFKP  226
Ct 38%   AKSDTMSPVELDNFKSRIRDIIEAQDINIYTP  203
Cg 35%   SKADTLTAQELQLFKSRIRQVIEAQEIAIFTP  198
```

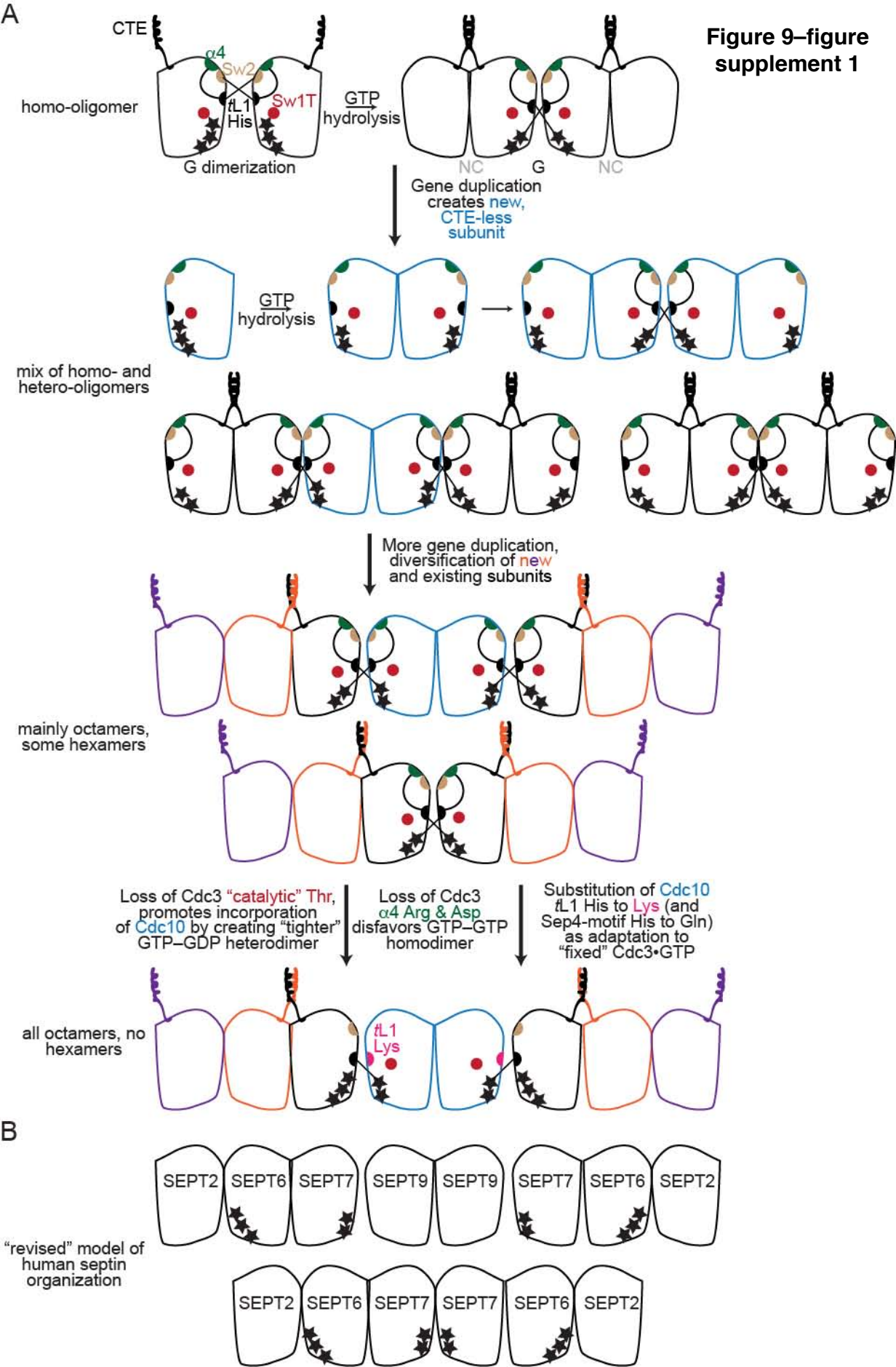

Figure 9–figure supplement 1